The definitive version of the text was subsequently published in: Quaternary Science Reviews, 2014, Volume 106, pp. 140-154, 15 December 2014, ISSN 0277-3791.

doi: 10.1016/j.quascirev.2014.06.009

Submitted version, accepted without substantial change

AMS ^{14}C and OSL/IRSL dating of the Dunaszekcső loess sequence (Hungary): chronology for 20 to 150 ka and implications for establishing reliable age-depth models for the last 40 ka

Gábor Újvári[a], Mihály Molnár[b], Ágnes Novothny[c], Barna Páll-Gergely[d], János Kovács[e,f], András Várhegyi[g]

[a]Geodetic and Geophysical Institute, Research Centre for Astronomy and Earth Sciences, Hungarian Academy of Sciences, Csatkai E. u. 6-8., H-9400 Sopron, Hungary

[b]Hertelendi Laboratory of Environmental Studies, Institute for Nuclear Research, Hungarian Academy of Sciences, Bem tér 18/C, H-4026 Debrecen, Hungary

[c]Department of Physical Geography, Eötvös Loránd University, Pázmány Péter sétány 1/c, H-1117 Budapest, Hungary

[d]Department of Biology, Shinshu University, Matsumoto 390-8621, Japan

[e]Department of Geology and Meteorology, University of Pécs, Ifjúság u. 6., 7624 Pécs, Hungary

[f]Environmental Analytical and Geoanalytical Research Group, Szentágothai Research Centre, University of Pécs, Ifjúság útja 20., H-7624 Pécs, Hungary

[g]Department of Environmental Engineering, Polláck Mihály Faculty of Engineering and Information Technology, University of Pécs, Rozmaring u. 17., H-7634 Pécs, Hungary

Corresponding author e-mail address (G. Újvári): ujvari.gabor@csfk.mta.hu

Abstract

As revealed by 18 AMS radiocarbon and 24 OSL/IRSL ages the Dunaszekcső loess-paleosol sequence is an excellent terrestrial record of paleoenvironmental change in the Carpathian Basin for the last 130 ka, with significant soil forming episodes during the Eemian interglacial (130 to 115 ka, MIS 5e) and in some subsequent MIS 5 stages, and distinct periods of loess accumulations during the MIS 4 and MIS 2. Charcoals from the sequence made it possible to test the accuracy of ^{14}C ages from mollusc shells. This approach revealed that ^{14}C ages from some gastropods having small shells (<10 mm) (*Succinella oblonga*, *Vitrea crystallina*) are statistically indistinguishable from the ages of charcoals, while others (Clausiliidae sp., *Chondrula tridens*) show age anomalies up to 600-800 years. OSL and pIRIR@290 ages are found to be consistently older, while post-IR OSL ages are younger than the ^{14}C ages from charcoals and molluscs by some thousands of years, except for pIRIR@225 ages that match the radiocarbon ages quite well. OSL and IRSL ages have scatters up to 7-10 thousand years within 40 ka, while charcoals and small molluscs yield consistent ages with relatively low variability. Beyond the observation that some small molluscs seem to yield reliable ^{14}C ages, calibrated 2σ age ranges of the radiocarbon data (ca. 500–800 years for 20 to 30 ka) are an order of magnitude narrower than those of the OSL/IRSL methods (1800 to 4000 years for 25 to 35 ka). Thus, for establishing chronologies within 40 ka, which are both accurate and precise enough to address issues like synchroneity of millennial-scale paleoenvironmental events across regions (e.g. North Atlantic and Europe), AMS radiocarbon dating of shells of specific loess molluscs and charcoals may probably be a powerful chronological tool. However, additional work is definitely required involving ^{14}C and OSL/IRSL dates from other loess sequences to further test the performance of these two supposedly robust chronometers.

Keywords: loess; paleosol; radiocarbon dating; OSL and IRSL dating; mollusc; Hungary

1. Introduction

Ice core oxygen isotope records reveal a succession of millennial scale warm-cold (Dansgaard-Oeschger, D-O) oscillations in air temperature over Greenland for the last glaciation (Johnsen et al., 1992; Dansgaard et al., 1993). As demonstrated by Bond et al. (1993), rapid sea surface temperature changes and massive iceberg discharges recorded in North Atlantic sediments are associated with the D-O events in Greenland ice cores in the last 90 ka. It seems to be reasonable to assume that temperature fluctuations of 7-13 °C between cold and warm stages over Greenland must have been associated with significant environmental changes in the entire North Atlantic, particularly in Europe (Johnsen et al., 1992). Indeed, millennial scale oscillations have been found in terrestrial records such as loess deposits in Europe (grain size: Vandenberghe and Nugteren, 2001; Rousseau et al., 2002; Shi et al., 2003; Rousseau et al., 2007; Antoine et al., 2009a,b; Stevens et al., 2011; Vandenberghe et al., in press; mollusc assemblages: Sümegi and Krolopp, 2002; Moine et al., 2008) and even in Asia (grain size: Porter and An, 1995; Xiao et al., 1995; Stevens et al., 2006, 2007; Sun et al., 2012). Grain size maxima have been suggested to correlate with D-O stadials, Heinrich events and high dust accumulation (Ca^{2+} concentration peaks) in Greenland (Rousseau et al., 2002, 2007; Antoine et al., 2009a,b), and Heinrich events and $\delta^{18}O$ minima in the GRIP (Shi et al., 2003; Porter and An, 1995) and maxima in the NGRIP ice cores (Sun et al., 2012). Such correlations and the investigation of synchroneity between events have mostly been based on tuned chronologies (Porter and An, 1995; Rousseau et al., 2002, 2007; Shi et al., 2003), partly resting on absolute ^{14}C and/or OSL/IRSL ages. The reasoning behind tuning is that sediment boundaries and proxy events must have been produced by major climate or environmental events, that they were recorded in many regions and multiple types of deposits in a (nearly) simultaneous manner, and these events can be used as isochrons to date individual archives (Blaauw, 2012). Of course, considerable risks exist behind this approach as the past behavior of separate or interacting climate systems is not exactly known and the evolution of each proxy archive is heavily dependent on a unique combination of climatic thresholds, environmental settings and internal variability (Winkler and Matthews, 2010). Thus, events can be expressed quite uniquely in different locations. This is why independent direct dating of loess appears to be the only means by which an effective chronology can be gained (Stevens et al., 2007), any pre-conceived ideas about the timing of certain proxy changes eliminated and a possible circular reasoning avoided (Blaauw, 2012). Consequently, only non-tuned and independent age-depth models of loess records can be used to assess the timing between climatic/environmental events across regions. At present, however, low resolution dating of loess sequences and age-depth models with uncertainties of millennial magnitude prevent us from a) determining whether abrupt climatic changes were regionally synchronous, b) investigating the regional response of climate and environment to a supposed common forcing, and c) quantifying leads and lags between regions in the North Atlantic and Europe over the last 60 ka, key objectives of the INTIMATE project (Lowe et al., 2008; Blockley et al., 2012). No doubt that aeolian loess deposits may serve as key terrestrial archives of millennial or even centennial scale environmental change (Stevens et al., 2007; Sun et al., 2012), although these records can only be fully utilized if their chronologies are refined. This means higher resolution dating of these sequences, at least at levels of 10-30 cm per dated sample, a resolution that has only recently been attained by few research groups in OSL dating of Chinese and Romanian loess (Stevens et al., 2006, 2007, 2008; Vasiliniuc et al., 2011; Timar-Gabor and Wintle, 2013) and in ^{14}C dating of East-Carpathian loess so far (Haesaerts et al., 2009). Additional problems are the low precision of luminescence ages and the general lack of organic macrofossils (e.g. charcoal) in loess that can reliably be dated using ^{14}C (Trumbore, 2000; Hatté et al., 2001). Other datable phases in loess are humic substances (humic acids), rhizoliths, mollusc shells and organic matter (McGeehin et al., 2001; Pigati et al., 2013; Gocke et al., 2014). The latter has been used for ^{14}C-dating of the Nussloch sequence in Germany by Hatté et al. (2001). Unfortunately, subsequent studies demonstrated that rejuvenation of organic matter in loess frequently occurs, thereby causing serious problems regarding the reliability of ^{14}C ages of loess organic matter (Gocke et al., 2010, 2011). Also the interpretations of humic acid ^{14}C ages are in many cases not straightforward, as these acids are often soluble in groundwater depending on the pH and act as contaminants, i.e. originate from younger vegetation and not from in situ plant decay (Ascough et al., 2011; Wild et al., 2013). Radiocarbon dating of rhizoliths (hypocoatings) that were formed by coating of plant roots by secondary carbonate (Klappa, 1980; Becze-Deák et al., 1997; Barta, 2011) proved that these phases are not syn-sedimentary (Pustovoytov and Terhorst, 2004; Gocke et al., 2011; Újvári et al., 2014a). Recently, promising leaf wax ^{14}C ages are published from a loess profile (Häggi et al., 2013), but this compound-specific radiocarbon dating is extremely time- and labor-intensive. Thus for a possible routine use, the only remaining phases to be dated from loess are mollusc shells, but these are usually regarded as unreliable material for ^{14}C-dating, as they may incorporate ^{14}C-deficient (or dead) carbon from the local carbonate-rich substrate during shell formation, thereby producing anomalously old ages by up to 3000 years (Rubin et al., 1963; Tamers, 1970; Evin et al., 1980; Goodfriend and Stipp, 1983; Goodfriend and Hood, 1983; Yates, 1986; Goodfriend, 1987; Zhou et al., 1999; Xu et al., 2011). However, most of these works were biased towards gastropods having relatively large shells (>20 mm) and recent studies by Brennan and Quade (1997) and Pigati et al. (2004, 2010, 2013) demonstrated that reliable ^{14}C ages can be obtained from small gastropods (shells <10 mm) that have largely been ignored in previous ^{14}C dating studies on molluscs.

Bearing all the problems and progress discussed above in mind, a dating framework has been started for the Dunaszekcső loess-paleosol sequence in Hungary to investigate how a reliable chronology, both accurate and precise enough to achieve objectives defined by the INTIMATE group, could be established. As we will demonstrate, our datasets appear to support the idea of using small gastropods for building ^{14}C-chronologies for the last 40 ka for loess, but also point to problems such as considerable discrepancies between ^{14}C and OSL, post-IR OSL and post-IR IRSL290 ages. Two sigma ranges of luminescence ages cover several thousands of years, while calibrated ^{14}C age ranges (2σ) are an order of magnitude lower (500-800 years) for 20 to 30 ka. Further, we provide a tentative chronology for the investigated sequence for 20 to 150 ka.

2. Material and methods

2.1. Study site and sampling

The studied loess-paleosol section is located at Dunaszekcső, Southern Hungary, on the right bank of the Danube river (46°05'25"N, 18°45'45"E, and 135 m a.s.l.; Fig. 1) and exposes glacial-interglacial sediments with a thickness of 17 m. Altogether 8 different lithological units can be distinguished in the studied wall starting from unit 1 (17.00-14.50 m) at the base of the sequence which is made up of homogeneous calcareous loess (Fig. 2). The contact between unit 1 and the overlying pedocomplex (represented by units 2, 3 and 4 between 14.50 and 12.30 m) is characterized by carbonate concretions (1-10 cm in diameter). This reddish-brown, 2.20 m thick pedocomplex is comprised of two brown soil horizons (units 2 and 4) out of which the upper one is less well-developed, and an intercalating yellowish-gray loess layer (unit 3). Unit 5 (12.30 to 11.00 m) is a grayish-yellow to brownish-yellow, relatively porous loess horizon (L1L2) with a gradual transition towards the underlying soil, while unit 6 (11.00-8.30 m) is an altered, weakly developed soil horizon (L1S1). Unit 6 is overlain by pale yellow, calcareous, sometimes sandy loess in a thickness of 6 m (unit 7, 8.30-2.30 m). The boundary between the loess horizon (unit 7, L1L1) and the overlying, dark brown chernozem soil (unit 8, 2.30-0.00 m) is sharp and the upper half of this modern soil (S0, Holocene) is heavily affected by anthropogenic activity.

In 2008, an enormous bank failure exposed the uppermost 15-20 m part of the ca. 70 m thick Quaternary loess-paleosol sequence at Dunaszekcső (Újvári et al., 2009), thereby allowing the sampling of a fresh profile. After cleaning of the sediment surface, altogether 7 samples were collected for luminescence dating throughout the profile at various depths down to the L2 loess unit (Fig. 2). This was done by pushing metal tubes into the loess-paleosols. Additional sediment samples from around the luminescence sampling holes were taken for gamma spectrometry. For ^{14}C-dating, loess cuboids with dimensions of 15 × 5 × 10 cm at depths of 4.00, 5.00, 6.00 m, and 15 × 5 × 7.5 cm (length-width-height) at depths of 8.20 and 8.25 m were prepared and cut from the L1 loess unit (Figs. 2 and 3). Sample blocks were subsequently disintegrated in the lab by soaking them in distilled water. Charcoals, rhizoliths and gastropod shells were extracted by washing the sediments through a 1 mm mesh sieve then dried at 50 °C and handpicked using gloves and pre-cleaned forceps to avoid modern carbon contamination. After being identified at the species (or family) level, shells were wrapped in Al-foil and put in closed plastic bags. Also the charcoal and rhizolith samples were handled and packed in a similar way, but separately from gastropod shells. The nomenclature of mollusc species follows Welter-Schultes (2012).

2.2. Radiocarbon dating

Gastropod shells, rhizoliths and charcoals were further pretreated in the new AMS laboratory of the Hertelendi Laboratory of Environmental Studies, Institute for Nuclear Research, Debrecen, Hungary (Molnár et al., 2013a). During this procedure charcoal fragments were treated using the standard acid-base-acid (ABA) method (Jull et al., 2006), i.e. in a sequence of 1N HCl, distilled water, 1M NaOH, distilled water, and then 1N HCl. After the final acid wash, the sample has been washed again with distilled water to neutral pH (4–5) and dried. Mollusc shells were ultrasonically washed and then all the surficial contaminations and carbonate mineral coatings were etched by using weak acid (2% HCl). Etching effectively removed ca. 20-30 percent of the shell materials that were dried and put into vacuum tight two finger reaction ampoules and dissolved by phosphoric acid. Subsequently, CO_2 was extracted by combustion and acidic hydrolysis of samples, further purified cryogenically and then graphitized (Molnár et al., 2013a). For testing the various organic and carbonaceous sample preparation procedures, some international ^{14}C reference materials from IAEA-C1 to C9 series with known ^{14}C activity have been prepared and measured together with the charcoal samples. All the ^{14}C measurements were done on the graphitized samples using a novel, compact radiocarbon AMS system (MICADAS) developed at the Paul Scherrer Institute and the ETH Zürich (Synal et al., 2007; Wacker et al., 2010), which was installed at the Hertelendi Laboratory of Environmental Studies, Debrecen in 2011 (Molnár et al., 2013b). Conventional radiocarbon ages were converted to calendar ages using OxCal online (version 4.2; Bronk Ramsey, 2009) and the IntCal13 calibration curve (Reimer et al., 2013). Calibrated ages are reported as age ranges at the 2 sigma confidence level (95.4%).

2.3. Luminescence dating

2.3.1 Equivalent dose determination

Luminescence samples, as mentioned above, were taken by pushing metal tubes into the previously cleaned wall, or if it was not feasible block samples were collected and only the light protected middle part of the material has been used for the luminescence preparation. All preparation steps were conducted under subdued red light and all samples were treated with 0.1 N HCl, 0.01 N $Na_2C_2O_4$ and 30% H_2O_2 to remove carbonate, clay coatings and organic matter. Subsequently, the polymineral fine grain fraction (4-11 μm) has been extracted from the sediments. 34% fluorosilicic acid (H_2SiF_6) was used for 5 days to remove feldspar grains from the polymineral fine grains to obtain a pure quartz fraction from 3 samples.

Luminescence measurements were performed using an automated Risø TL/OSL-DA-20 reader at the Department of Physical Geography, Eötvös Loránd University. The reader is equipped with a bialkali EMI 9235QB photomultiplier tube, IR diodes (λ=875 nm), blue LEDs (λ=470 nm) and a $^{90}Sr/^{90}Y$ β-source. A 7.5 mm Hoya U-340 filter was placed between the photomultiplier and the aliquots to allow measurement of the emitted UV wavelength (280–380 nm) for quartz minerals. For the potassium-feldspars, Schott BG-39 and BG-3 filters were placed in front of the photomultiplier to measure the blue light emission during IRSL analyses, transmitting wavelengths between 350 and 420 nm.

2.3.1.1 Quartz dating – OSL and post-IR OSL methods

OSL SAR protocol (Murray and Wintle, 2000) has been applied for fine grained quartz to determine the equivalent dose (D_e) of three samples. The purity of quartz samples was checked by infrared (IR) stimulation. In case of any observable feldspar contamination the aliquot has been rejected and not used in further evaluation. Blue stimulation for 40 s at 125°C was applied during the measurements. An extra hot-bleach step (blue stimulation at 280°C for 40 s) was done to reduce the recuperation (Murray and Wintle, 2003). Dose-recovery tests on different preheat temperatures (240, 260 and 280 °C) were carried out to determine the best preheat conditions. Dose-recovery test resulted in rather poor dose-recovery ratios in each temperature, ranging between 1.06 and 1.26, although the samples were mounted into cups for the better heat transfer. Therefore, a second dose-recovery test was done on sample Dsz 1, but this time the given dose was added on top of the natural dose (Schatz et al., 2012). This second, repeated dose-recovery test resulted in much better ratios ranging from 0.97 to 1.03. For further measurements a preheat of 260°C and a cut-heat of 220°C were selected. Early or late background subtraction had no effect on the results. Thus, D_e values of the samples were calculated by integrating the 0-1 s region of the OSL decay curve and the final 5 s of stimulation was subtracted as background. All dose-response curves were fitted using a saturating exponential function.

The post-IR OSL protocol was applied on polymineral fine grain samples, as a comparison with the quartz OSL and feldspar post-IR IRSL measurements. In this protocol IR bleaching is used prior to blue stimulation in order to bleach any signal coming from the feldspar. As a result, the subsequent OSL signal is expected to be dominated only by quartz. The IR bleaching was conducted at 200°C for 100 s. Extra hot-bleach steps (infrared stimulation at 280°C for 100 s and subsequently blue stimulation at 280°C for 100 s) were used to reduce the recuperation (Murray and Wintle, 2003). A preheat of 220°C for 10 s and a cut-heat of 160°C were chosen for the D_e measurement.

2.3.1.2 Feldspar dating – post-IR IRSL225 and 290 (pIRIR@225 and pIRIR@290) protocols

The conventional IRSL dating of feldspars would be a useful tool for dating well-bleached Middle and Late Pleistocene loess. However, due to anomalous fading of feldspars, this method can produce significant age underestimations (Wintle, 1973). Recently, a new method is developed using the post-Infrared Infrared Stimulated Luminescence (post-IR IRSL) signal of feldspar (Thomsen et al., 2008; Buylaert et al., 2009, 2012; Thiel et al., 2011), which shows negligible fading, therefore additional fading correction is not needed (Huntley and Lamoth, 2001). First, an IR stimulation of 200 s at 50 °C, then an elevated temperature IR stimulation of 200 s either at 225 °C or at 290 °C (depending on the applied protocol) is used to measure the IRSL and the subsequent post-IR IRSL signals of the feldspar samples. Following the measurement protocol described in Buylaert et al. (2009) and Thiel et al. (2011) a preheat of 250 °C or 320 °C for 60 s was applied prior to the stimulations. An extra hot-bleach step (IRSL stimulation at 290°C or at 325°C for 100 s) was done for the samples to reduce recuperation (Murray and Wintle, 2003). For post-IR IRSL signals the D_e values were obtained by integrating the first 2.5 s of the IRSL decay curve with a subtraction of the final 100 s of stimulation to remove the background. All dose-response curves were fitted using a sum of two saturating exponential function. Dose-recovery test was carried out on all samples after daylight bleaching by subtracting the residual dose and dose-recovery ratios range between 0.97±0.01 and 1.03±0.01 for the pIRIR@225 protocol and between 1.09±0.04 and 1.30±0.04 for the pIRIR@290 protocol, respectively. Subsequently, the dose recovery test was repeated, but at this time the given dose was administered on top of the natural dose and the natural signal was subtracted from the measured recovered dose in the calculations. This process improves the dose-recovery results (Schatz et al., 2012), and decreased the dose-recovery ratios for both protocols. It must be noted, however, that the dose recovery ratios still exceed the accepted limit for the pIRIR@290 protocol (range from 1.13±0.03 to 1.23±0.15). Small residual signal (~5 Gy) was observed after a 1 day daylight bleaching, hence this value has not been subtracted from D_e (Murray et al., 2014). In general, the pIRIR@290 signals are less affected by fading (Thiel et al., 2011), however, in our fading tests both methods (pIRIR@225 and pIRIR@290) resulted in negligible fading rates: 0.61 and 0.13 %/decade, respectively, therefore fading correction was not applied.

2.3.2 Dose-rate determination

Dose rates were obtained from the potassium, uranium and thorium contents, as measured by gamma spectrometry in the accredited laboratory at Mecsekérc Environment Protection Co. For gamma spectrometric analyses of loess/soil samples an Oxford HPGe semiconductor detector multichannel (8k) system was used (detector efficiency 40%). Samples were homogenized and powdered below 100 μm grain size and subsequently dried at 105 °C and hermetically sealed in Marinelli sample beakers. All the measurements were performed after the Ra-Rn radioactive equilibrium having been reached. A 10 cm thick lead chamber coated with 1 mm copper layer inside served as shielding of background radiation and to supress the Roentgen component. A measurement time (live) of ≥50,000 s was applied. Evaluation of spectra was performed using the Oxford Gamma Vision software package. Instead of using the most prevalent detector efficiency method, the more accurate relative method was applied for the quantitative evaluation of gamma spectra, using calibration standards with the same matrix and measurement geometry as those of the samples. The main gamma emitters of ^{238}U, ^{235}U, ^{232}Th radioactive decay series and ^{40}K were evaluated using the individual photo-peak(s) of each radionuclide. Activity concentrations of ^{235}U, ^{234}Th, ^{226}Ra, ^{214}Pb, ^{214}Bi, ^{210}Pb, ^{228}Ac, ^{212}Pb, ^{212}Bi, ^{208}Tl, and ^{40}K have been given for each sample. Total radioactivity of samples expressed in ^{226}Ra equivalent and radioactive equilibrium factor between ^{226}Ra/^{238}U were also calculated. A potassium content of 12.5±1% (Huntley and Baril, 1997) was applied to the K-rich feldspar fraction to account for the internal dose rate. An average a-value of 0.08±0.02 (Rees-Jones, 1995) was used for the feldspar IRSL age calculations, while 0.06±0.02 (Schmidt et al., 2010) and 0.04±0.02 (Rees-Jones, 1995) were applied for the quartz post-IR OSL and OSL age calculations. The cosmic radiation was corrected for altitude and sediment thickness (Prescott and Hutton, 1994), assuming a water content of 15±5% for samples down to a depth of 12 m and 20±5% for samples below it. The use of water contents in this range is justified by soil moisture values from 6 to 21% observed in a Serbian loess profile (Stevens et al., 2011). Dose rate conversion is based upon the factors of Adamiec and Aitken (1998).

3. Results

3.1. Radiocarbon ages from rhizoliths, charcoals and mollusc shells

Measured ^{14}C activities of international reference materials (IAEA-C1 marble, C2 travertine, and C9 wood) showed excellent agreement with the reference values (Table S1), thereby providing evidence for the appropriateness of sample preparation and AMS ^{14}C analyses procedures at the Hertelendi Laboratory of Environmental Studies. All the rhizoliths from three loess samples collected at depths of 4.00, 5.00 and 6.00 m yield Holocene ages (Fig. 3 and Table 1). This means that rhizoliths cannot be used to date loess sedimentation, so these ages are not considered further in this study.

Charcoals can be found as dispersed fragments in a 12-15 cm thick sediment layer at a depth of ca. 8.15 to 8.30 m in the studied section (Figs. 2 and 3). Two independent ^{14}C ages are available from these charcoal fragments, 25568±105 and 26101±110 ^{14}C yr BP (Dsz-Ch1 and 2 samples, Table 1) yielding a mean conventional age of 25835±380 (^{14}C yr BP) that leads to a 2σ age range of 29190 to 30870 cal BP after calibration. AMS radiocarbon dating of 7 mollusc shells from the two separate sub-samples (8.20 and 8.25 m) of the given charcoal horizon provided ages from 15844±56 (*Trochulus hispidus=Trichia hispida*, Dsz-Ch1) to 26979±126 ^{14}C yr BP (Clausiliidae sp., Dsz-Ch1). The apparently young ^{14}C age of *Vitrea crystallina* (20724±111 ^{14}C yr BP) from sample Dsz-Ch2 originates from analytical issues (low current and problematic background correction due to very small sample size, i.e. 0.2 mg C), while the discrepant age of *T. hispidus* (15844±56 a BP) is attributed to open-system behavior. Excluding these two anomalous data, ^{14}C age anomalies, using 1 sigma errors, have been found in a range of -263±165 to +878±167 ^{14}C yrs, compared to the respective charcoal ages from samples Dsz-Ch1 and 2 (Table 1). (Note that ^{14}C ages of shells are compared here to the charcoal ^{14}C age coming from the same sub-sample of the charcoal horizon). *Succinella (Succinea) oblonga* shows the lowest age anomaly (41±167 ^{14}C yr), while Clausiliidae sp. reveals the highest (878±167 ^{14}C yr). A negative age anomaly of -263±165 ^{14}C yr is observed for *V. crystallina* implying that this shell appears to be slightly younger than the respective charcoal from sample Dsz-Ch1. In terms of calibrated age ranges, all of them overlap within 2σ errors with the charcoal ages except for the two anomalous ages mentioned above (Fig. 4). Out of the analyzed shells those of *S. oblonga* and *V. crystallina* show the largest overlaps in age with charcoals.

Although upper parts of the studied loess profile are devoid of charcoals, there are some ^{14}C ages from species having smaller (*T. hispidus* and *S. oblonga*) and larger shells (*A. arbustorum*). These are available at three depths (4.00, 5.00 and 6.00 m) for comparison with each other and the OSL/IRSL ages (Table 1, Figs. 2 and 5). At a depth of 6.00 m, *T. hispidus* gave a slightly younger raw ^{14}C age (22332±80 ^{14}C yr BP) than *S. oblonga* (23036±88 ^{14}C yr BP) with a difference of 704±119 ^{14}C yrs. At depths of 5.00 and 4.00 m, *T. hispidus* provided radiocarbon ages of 19656±76 and 18678±68 ^{14}C yr BP that proved to be younger than the ^{14}C ages of 20504±79 and 20585±75 ^{14}C yr BP from *A. arbustorum*. Age differences for the same depths are 848±110 (depth: 5.00 m) and 1907±101 ^{14}C yrs (depth: 4.00 m). Although the 2 sigma calibrated age ranges for *S. oblonga* and *T. hispidus* from a depth of 6.00 m are very close to each other, they do not overlap within 2σ uncertainties and this holds true for the rest of the shell radiocarbon ages from depths of 5.00 and 4.00 m (Fig. 5).

3.2. Quartz OSL and K-feldspar IRSL ages

Results of gamma spectrometry are listed in Table 2 and these values have been used to calculate total dose rates shown in Tables 3 and 4. They range from 2.44±0.15 Gy ka^{-1} to 2.91±0.17 Gy ka^{-1} for fine-grained quartz, from 2.60±0.15 Gy ka^{-1} to 3.54±0.18 Gy ka^{-1} for fine-grained polymineral post-IR OSL signals and they are similar to those obtained from other East Central European sites (Schmidt et al., 2010, 2011; Fitzsimmons and Hambach, in press). The total dose rates for feldspars range from 2.76±0.11 Gy ka^{-1} to 3.75±0.13 Gy ka^{-1}, values that overlap with those previously found for other Hungarian loess-paleosol profiles (Novothny et al., 2002, 2011; Schatz et al., 2012; Thiel et al., 2014). Shapes of decay curves for the OSL, post-IR OSL and post-IR IRSL measurements significantly differ from each other, but all of them show the typical shape of a pure quartz, a mixed quartz-feldspar and a feldspar signal, respectively (Fig. S1).

Considering the aeolian origin of these samples well bleached minerals are expected, which has been confirmed by the low residual values and relatively minor inter-aliquot variations. Consequently, the mean of the calculated D_e values are taken for each method. Quartz OSL are measured only for 3 samples (Dsz 1, 4, 7) and yielded ages ranging from 29.9±1.7 ka to 105±6 ka (Table 3). While the post-IR OSL ages from the polymineral fraction range from 19.3±1.2 ka to 102±7 ka (Table 3), pIRIR@225 ages vary from 25.0±0.9 ka to 164±7 ka, and pIRIR@290 ages cover an age range of 31.7±2.0 ka to 154±8 ka (Table 4). Comparing the quartz and feldspar ages for the uppermost sample (Dsz 1), the OSL and pIRIR@290 ages overlap within 1σ errors, while the pIRIR@225 and post-IR OSL methods yield much younger ages. For samples Dsz 2, 3 and 4, the post-IR OSL, pIRIR@225 and pIRIR@290 ages significantly differ from each other with post-IR OSL ages being consistently the youngest, while pIRIR@290 ages the oldest ones. For the lowermost three samples (Dsz 5, 6, 7), the pIRIR@225 and pIRIR@290 ages are overlapping and significantly older than the post-IR OSL ages. Regarding the oldest sample (Dsz 7), both the quartz OSL and polymineral post-IR OSL ages underestimate the post-IR IRSL ages. This observation is not surprising considering the lower saturation limit of the quartz OSL signal (~200 Gy; Wintle and Murray, 2006). The luminescence datasets are consistent from a stratigraphic point of view (Fig. 2), except for one sample (age reversal, Dsz 6).

4. Discussion

4.1. Reliability of charcoal and mollusc shell ^{14}C ages from loess

Charcoal is produced during pyrolysis accompanying the incomplete combustion of woody plant tissues under conditions of restricted oxygen (Bird, 2006; Bird and Ascough, 2012). During this process lignocellulose structures degrade leading to the formation of chemically stable aromatic rings and, with increasing pyrolysis temperatures, to a higher abundance of ordered microcrystalline domains with higher chemical stability (Bird and Ascough, 2012). Thus, charcoal is thought to be highly resistant to post-depositional alteration and relatively chemically inert (Preston and Schmidt, 2006). There is a growing body of evidence, however, that charcoal is prone to alteration and degradation and can finally be lost from the burial environment through oxidation processes (Rebollo et al., 2008; Braadbart et al., 2009; Ascough et al., 2011). Moreover, degraded, partially oxidized charcoal can readily adsorb a range of chemical contaminants such as humic substances which may be of a different ^{14}C age than the charcoal from the same sedimentary horizon (Ascough et al., 2011; Wood et al., 2012). Obviously, this exogenous carbon must be removed prior to dating to obtain a robust age and for this purpose the most common technique has been the ABA pretreatment that involves sequential washing with acid-base-acid for the removal of carbonates, humic acids, and finally the atmospheric CO_2 absorbed during the base step (Bird, 2006). It has been demonstrated however, that for samples older than ca. 30-40 ka the ABA method was not capable of removing all contaminations from charcoals in comparison with the acid-base-oxidation with stepped combustion (ABOX-SC) technique (Bird et al., 1999; Turney et al., 2001; Bird et al., 2003; Wood et al., 2012; Bird et al., 2014). In fact, the problem that ABA does not remove contamination as efficiently as ABOX-SC become critical for old samples (40-60 ka) when only a small amount of modern carbon may have a significant impact on ^{14}C ages (Bird and Ascough, 2012). For younger samples (<30-40 ka), the ABA and ABOX-SC pretreatments give statistically indistinguishable ages in most cases (see Turney et al., 2001; Higham et al., 2009; Douka et al., 2010). Consequently, we believe that our ABA treated charcoal ages that are much younger than 40 ka are reliable and accurate and can be used as references in comparison with mollusc shell ^{14}C ages. This conclusion is further confirmed by the fact that two different charcoal fragments were dated from two independent sediment blocks and still they ages differ only by ca. 500 years (25568±105 and 26101±110 ^{14}C yr BP).

Carbon in mollusc shell carbonate originates from atmospheric CO_2, food, water and carbonate rocks and it incorporates into the shell through a variety of direct and indirect pathways (for detailed overviews see Goodfriend and Hood, 1983; Balakrishnan and Yapp, 2004; Pigati et al., 2010). Since ^{14}C activities of live plants and water (dew, precipitation) available for consumption by terrestrial gastropods are in equilibrium with atmospheric carbon (about 100 percent modern carbon, pMC), loess molluscs that obtain their shell carbon from plants, water and air should yield reliable ^{14}C ages, assuming these shells behaved as closed systems after burial (Pigati et al., 2010). This holds true for gastropods that consume decaying plant litter, as time elapsed between plant death and consumption is usually short (few yrs, Pigati et al., 2010). At the same time, the incorporation of carbon from old (pre-Quaternary) carbonates, typically having ^{14}C activities of 0 pMC, presents a significant problem for radiocarbon dating of loess mollusc shells. This old carbonate was readily available for molluscs that lived on the loess steppe, as primary detrital calcite and dolomite are abundant in loess deposits (Pye, 1983; Pye, 1995; Újvári et al., 2008). Thus, it is of crucial importance to identify mollusc taxa that do not incorporate dead carbon (or only in very low amounts) into their shells, thereby gaining accurate ^{14}C ages for establishing reliable loess chronologies. Previous studies have found that fossil shells of some small gastropods (genera *Catinella*, *Cochlicopa*, *Columella*, *Discus*, *Euconulus*, *Nesovitrea*, *Punctum* and *Succinea*) meet this requirement and are expected to yield reliable ^{14}C ages irrespective of the local geological substrate (Pigati et al., 2004, 2010, 2013).

In our study we adopted the approach of testing mollusc shell-based ^{14}C age accuracy against ^{14}C ages of charcoals (Tamers, 1970; Zhou et al., 1999; Pigati et al., 2010) and found that indeed minute gastropods provide ^{14}C ages that are in good agreement with those from charcoals. *S. oblonga* shell was found to give the most accurate age with an age anomaly of 41±167 ^{14}C yrs, if its conventional radiocarbon age (26142±125 ^{14}C yr BP) is compared with the charcoal radiocarbon age (26101±110 ^{14}C yr BP) from the same sample (Dsz-Ch1; Table 1, see Fig. 4

for a comparison based on calibrated age ranges). Taking the pooled mean conventional ^{14}C age of 25835±380 ^{14}C yr BP from the two charcoals as a reference, *V. crystallina* (from sample Dsz-Ch1) showed the best match (25838±110 ^{14}C yr BP) and for which an age anomaly is meaningless (3 ^{14}C yrs). However, if compared with the charcoal age of 26101±110 ^{14}C yr BP from the same sample (Dsz-Ch1), a slightly higher and negative age anomaly (-263±165 ^{14}C yrs) is observed. Unfortunately, shells of *V. crystallina* from sample Dsz-Ch2 gave anomalous ages due to analytical problems. (This species has tiny and very thin shells that yielded a low amount of sample, only 0.2 mg C in this case, resulting in low current and problematic background correction.) Anyway, the conventional radiocarbon ages and even more the strongly overlapping 2σ age ranges confirm previous findings of Pigati et al. (2010, 2013) that the genus *Succinea* yield reliable ^{14}C ages and it seems likely that *V. crystallina* can also be used for radiocarbon dating of loess sediments with good accuracy. Other species like *Chondrula tridens* and the family Clausiliidae (these shells could not be reliably identified at the species level in lack of apertures) revealed age anomalies of 750±161 ^{14}C yrs (*Ch. tridens*), 545±166 and 878±167 ^{14}C yrs (Clausiliidae sp. from Dsz-Ch2 and Ch1) (Table 1). Also the calibrated age ranges are much less overlapping (Fig. 4). Interestingly, Clausiliidae sp. from sample Dsz-Ch2 gave a radiocarbon age of 26113±129 ^{14}C yr BP matching very closely the charcoal age of 26101±110 ^{14}C yr BP from sample Dsz-Ch1 (see also Fig. 4 for 2σ age ranges). Clearly, the formation of the 10-15 cm thick loess layer containing the charcoal fragments and mollusc shells could last some hundreds of years depending on dust influx and sedimentation rates. Further, these organic macrofossils may have been originated from subsequent events of biomass burning that resulted in the measured ca. 500 years age difference between the two charcoal fragments. Another explanation is that the purity of the two fragments was different after the ABA treatment and the observed small age difference is due to remaining contaminants (Alon et al., 2002). As the size of dated charcoal fragments were in the 5-10 mm range their vertical translocation in such a fine grained sediment like loess seems unlikely. Nevertheless, these factors mentioned above introduce additional uncertainty in comparisons between charcoal and mollusc shell derived ^{14}C ages.

As for the upper part of the studied loess section where charcoals are absent, *T. hispidus* gave comparable ages with *S. oblonga* at a depth of 6.00 m with an age difference of ca. 670 years. Considering that *S. oblonga* yields mostly accurate and sometimes slightly older ages than the real age of sedimentation (Pigati et al., 2010 and this study), the given loess layer should have formed at around 27000 to 27300 cal BP. For depths of 5.00 and 4.00 m, *A. arbustorum*, a large taxon, gave much older ages than *T. hispidus* (ca. 900 to 2000 years differences, Table 1, Figs. 2 and 5) and presents an age reversal, too. It is supposed based on our ^{14}C age datasets that the true ages of sedimentation at these depths may be placed closer to the ages provided by *T. hispidus*, implying a limestone effect on *A. arbustorum* that leads to anomalously old ages. In contrast to this, Sümegi and Hertelendi (1998) found that *A. arbustorum* shows only slight age anomalies (ca. 200 yr) compared with bone collagen ^{14}C ages. Regarding habitat preferences and dietary habits literature puts forward that *T. hispidus* lives in various damp habitats, in summer it climbs plants and stinging-nettles and likely feeds on these plants, while *A. arbustorum* feeds on green herbs, dead animals and faeces (Proćków, 2009; Welter-Schultes, 2012). Whether these differences in dietary habits may lead to any excess of dead carbon intake or not is unclear. In any case, eating of dead plants indeed may not cause a significant ^{14}C-deficiency in shells as surmised by Pigati et al. (2010), as *S. oblonga* feeds on green algae and rotting parts of plants (Welter-Schultes, 2012) and still yields reliable ^{14}C ages.

So far the best theory to explain the difference in dead carbon incorporation between small and large taxa has been the Ca-limiting hypothesis (Pigati et al., 2010) that was partly raised by Goodfriend (1987) in the context of ground- versus plant-dwelling species. In most settings, calcium can be found in plants and water in low amounts and small taxa can more easily satisfy their Ca demands than larger taxa. For this latter group it is likely more difficult to obtain enough calcium and they have to consume carbonate rocks to supplement their Ca intake during shell formation (Pigati et al., 2010), thereby incorporating ^{14}C-defficient carbon into their shells. Data presented by Xu et al. (2011) lends further support for tha Ca-limiting hypothesis in terms of dwelling behavior, as they found that ground-dwelling *Bradybaena*, for which Ca is continuously available, revealed much smaller age anomalies than other species inhabiting grasses or trees.

4.2. Reliability of OSL-IRSL ages from a luminescence viewpoint

As mentioned above, the first OSL dose-recovery tests resulted in rather poor dose-recovery ratios in each temperature, ranging between 1.06 and 1.26, despite the fact that the samples were mounted into cups for better heat transfer. Such a problem has been observed for other Hungarian loess samples, too (Schatz et al., 2012). Admittedly, failure of this basic internal test of the protocol implies that OSL ages of these samples are probably unreliable. This is why a second dose-recovery test was done on sample Dsz 1 by adding the given dose on top of the natural dose (Schatz et al., 2012) and it resulted in much better ratios ranging from 0.97 to 1.03. Therefore, we conclude that the quartz OSL age of sample Dsz 1 can be regarded as reliable. Since the OSL signal reaches its saturation limit at ~200 Gy (Wintle and Murray, 2006) it cannot be used as a robust chronological tool around or beyond it. For the studied samples this saturation limit is approached in sample Dsz 4, therefore only the OSL age of Dsz 1 is acceptable and the OSL age of Dsz 7 is clearly an underestimation due to saturation and can only be regarded as a minimum age. As the OSL age of Dsz 4 is close to the saturation limit it may be slightly underestimated. In a comparison of the post-IR OSL dataset with that of quartz OSL it is observed that the post-IR OSL ages are much younger than the quartz OSL ages. This is probably due to feldspar contamination which may not properly be eliminated from the OSL signal by the previous IR bleaching (except sample Dsz 7). Such a feldspar contamination results in post-IR OSL age underestimations due to anomalous fading that is not measured and corrected in this case.

For samples Dsz 1 and 4, pIRIR@290 ages are similar or close to quartz OSL ages, therefore it is concluded that the pIRIR@290 method provides a powerful and reliable tool to date older samples for which the quartz OSL signal saturates. The pIRIR@225 ages appears to be slightly underestimated compared to the pIRIR@290 ages for the younger samples (Dsz 1, 2, 3, 4), although their slightly higher fading rates (still below 1%/decade) would not cause such a discrepancy. At the same time, there is a remarkable consistency between pIRIR@225 and pIRIR@290 ages for the older samples (Dsz 5, 6, and 7).

4.3. Discrepancies between ^{14}C and OSL/IRSL ages and possible reasons

Since both ^{14}C and luminescence ages are available from a depth of 4.00 m these data can be directly compared. Two species of molluscs (*T. hispidus* and *A. arbustorum*) yield calibrated 2σ ^{14}C age ranges of 22370 to 22740 and 24470 to 25120 cal BP that are consistently younger by several thousands of years than the OSL and pIRIR@290 2σ age ranges (from 26.4 to 35.7 ka) and older than post-IR OSL age ranges (16.9 to 21.7 ka; sample Dsz 1 in Tables 3 and 4). At the same time, the 2σ age range of 23.2 to 26.9 ka provided by the pIRIR@225 method overlaps with the calibrated ^{14}C age range yielded by *A. arbustorum*. However, this latter age range is much narrower (Fig. 5). In comparison with *T. hispidus*, there is no overlap between the 2σ age ranges. As discussed above, *A. arbustorum* likely gives too old ages due to dead carbon incorporation, thus it cannot be excluded that the pIRIR@225 method gives slightly older ages than the true age of sedimentation. In such a case, it seems to be a difficult task to decide which ages are more accurate or in other words which ages (^{14}C or OSL/IRSL) best reflect the real age of sedimentation. Unfortunately, additional independent age data are not available as rhizoliths gave Holocene radiocarbon ages and their ^{230}Th-U dating failed to yield any ages due to high ^{232}Th contaminations. The only way to evaluate this or at least to gain some insight into the problem is the use of charcoal ^{14}C ages as references. As discussed in detail in the previous sub-chapter (4.1), evidences that small gastropods reveal no or only minor age anomalies in comparison with charcoal ^{14}C ages are growing, so they expect to yield the real age of sedimentation. Another argument in favor of charcoal and mollusc shell ^{14}C ages is their relatively high consistency at depths of 8.20 and 8.25 m (see Fig. 4). Despite the fact that these phases have very different origin and genesis, still they yield overlapping ages. A comparison of charcoal ^{14}C age ranges from depths of 8.20 (29960–30780 cal BP) and 8.25 cm (29350–30150 cal BP) with those provided by the OSL/IRSL methods from a depth of 7.75 m (Tables 1 and 3, and Figs. 2 and 4) suggests that pIRIR@290 ages (30.3–37.1 ka) overestimate the real age of sedimentation, while pIRIR@225 age ranges (26.3 to 30.8 a) likely cover the real age, provided that charcoal ages are accurate. Post-IR OSL ages are way too young (20.4 to 26.6 ka) in such a comparison.

A further essential observation is that age discrepancies between ^{14}C and OSL/IRSL ages are found to be much larger for younger samples (depth: 4.00 m) than for older ones (depths 7.75 and 8.20-8.25 m, Tables 1, 3, and 4). Similar features can be recognized in the chronological data of both the Süttő and Tokaj (Patkó-quarry) loess-paleosol sections in Hungary (Sümegi and Hertelendi, 1998; Novothny et al., 2009, 2011; Schatz et al., 2012). Possible reasons for OSL and IRSL ages to be too old are high water contents (15±5%) in the luminescence age calculations and that previous luminescence signal has not completely been removed during the short distance Aeolian transport from alluvial fans (Újvári et al., 2008; Újvári et al., 2012). However, considering the good agreement between OSL and pIRIR@290 ages insufficient bleaching seems to be unlikely (Murray et al., 2012; Thiel et al., 2014). Also extremely low

(<4%) water contents, that would otherwise result in luminescence ages close to the ^{14}C ages, are unrealistic in the light of measured data from a Serbian loess profile by Stevens et al. (2011).

4.4. Accuracy and precision of ^{14}C-OSL/IRSL ages and implications for creating age-depth models for the last 40 ka in an INTIMATE context

Previous attempts at synchronizing and correlating paleoenvironmental events in the North Atlantic and those recorded in loess assumed that these climatic/environmental episodes were caused by a shared process and most of the loess chronologies were tuned, based on plausible assumptions, to SPECMAP (Porter and An, 1995) and/or ice cores (Rousseau et al., 2002, 2007; Shi et al., 2003), partly controlled by some independent absolute age data. Obviously, nothing can be implied about any synchroneity, leads or lags between tuned events, as stressed by Blaauw (2012), thus non-tuned age-depth models are required for investigating synchroneity of abrupt climatic events. In a recent study by Sun et al. (2012), the authors established an independent, OSL-based chronology and found broad correlations between the East Asian winter monsoon and temperature variations in Greenland over the past 60000 years that, as they inferred, suggests a common forcing. Their proxy interpretations and correlations rest on ca. 40 OSL ages having 1σ uncertainties of 400 to 3500 years for a time span of 10 to 60 ka (relative 1σ error: 4 to 6 %). This problem has already been recognized by Porter and An (1995) when creating age-depth models for sections on the Luochuan loess platform based on thermoluminescence ages with relative 1σ errors of 9 to 18%. Since then considerable progress has been made in the field of luminescence dating (Lian and Roberts, 2006; Wintle, 2008), even though 1σ age errors of OSL ages for e.g. the Nussloch loess sequence in Germany range from 1500 to 9900 years (relative 1σ: 7 to 16%) for a time span of 19.8 to 61.3 ka (Lang et al., 2003; Tissoux et al., 2010; Kadereit et al., 2013). In our study, uncertainties (1σ) associated with OSL, post-IR OSL, pIRIR@225 and pIRIR@290 ages vary between a minimum of 900 (pIRIR@225, Dsz 1) up to 8000 years (pIRIR@290, Dsz 7) for a time interval of 25 to 156 ka (Table 3). Relative 1σ errors range from 3.7 to 5.1% that can be considered as excellent within the family of luminescence dating methods. The 2σ age ranges of the OSL/IRSL methods vary between a minimum of 3700 years (pIRIR@225, Dsz 1) and a maximum of 32000 years (pIRIR@290, Dsz 7). In a comparison with calibrated radiocarbon age ranges (ca. 500–800 years; Table 1, Figs. 2 and 4), however, it is immediately clear that these 2σ age ranges of OSL/IRSL are an order of magnitude larger. In an attempt at minimizing age model uncertainties to achieve INTIMATE objectives defined above ^{14}C ages undoubtedly outcompetes OSL/IRSL ages within 40 ka, if they are accurate. Evidences presented and discussed above (subchapters 4.1 and 4.3) lend support that ^{14}C ages provided by some minute gastropods are accurate within ca. -300 to +300 ^{14}C years. However, this additional uncertainty (i.e. beyond the uncertainty of the ^{14}C age data itself) must be taken into account in subsequent age-depth modeling studies based on mollusc shell ^{14}C ages from loess. After this effect having been considered, the estimated cumulative 2σ age ranges of ca. 800-1000 years for 20 to 30 ka (obviously depending on the number, quality and scatter of ^{14}C ages from the section) are comparable to the 2σ chronological uncertainties (ca. 600 to 900 years) with which the timing of GS and GI events are known for the same interval from ice cores (Andersen et al., 2006; Rasmussen et al., 2006; Svensson et al., 2008; Blockely et al., 2012).

It is concluded based on our datasets that reliable, relatively high precision chronologies can be established using ^{14}C ages of small molluscs and charcoals for the last 40 ka. Of course, further tests and work is clearly needed to confirm this finding. As both approaches (^{14}C and OSL/IRSL) yield useful ages and valuable insights into the timing of paleoenvironmental events the best practice would be to apply them together in order to cross-check and evaluate age accuracies. In our study pIRIR@225 ages are found to be closest to ^{14}C ages, but this may be a site-specific feature and also requires further testing. Further, as stressed by Telford et al.

(2004), accurate and high precision ^{14}C chronologies require high numbers of AMS radiocarbon dates and timing of events are probably better constrained by dating them directly, i.e. with dates immediately above and below the event horizon, than by age-depth models. Finally, the full use of time synchronous markers such as tephra horizons and geomagnetic excursions should be made (Blockley et al., 2012; Rolf et al., 2014). Indeed, such chronologic/stratigraphic markers may provide an independent basis for the direct correlation of events in last glacial loess of some regions (Veres et al., 2013; Fitzsimmons et al., 2013) and using them age-depth models can be further improved.

4.5. Chronology of the section

According to the ^{14}C ages the deposition of loess between 8.30 and 4.00 m took place from ca. 30 to 22 ka, possibly during cold phases occurred in the North Atlantic (GS-5 to GS-2c; Blockley et al., 2012), in broad agreement with significant loess formation in Serbia and Croatia (Marković et al., 2008; Galović et al., 2009; Antoine et al., 2009a; Bokhorst et al., 2011; Stevens et al., 2011). It is worth mentioning here, however, that some of these studies published ages that are based on the old, feldspar IRSL approach without fading correction and these ages cannot be directly compared with our new IRSL ages from the Dunaszekcső section. Nevertheless, the considerable loess accumulation from 30 to 22 ka is just one scenario that is based on ^{14}C ages, while another one is put forward by the OSL and pIRIR@290 ages that are regarded as the most reliable ages from a luminescence viewpoint and these ages range from ca. 36 to 26 ka (Tables 3 and 4). However, this latter period defined by OSL and pIRIR@290 ages was punctuated by many warmer interstadials (GI-7 to 3) that, if North Atlantic climate would have a substantial impact on that of East Central Europe, would not be favorable for considerable loess formation in the studied region. These observations cast at least some doubt on previous inferences made on OSL/IRSL ages from the Paks loess profile that significant loess accumulation took place in Hungary during MIS 3 and/or close to the transition to MIS 2 (Thiel et al., 2014).

Regarding the lower part of the sequence between 15.35 and 8.30 m, OSL and IRSL data are available at five depths ranging in ages from 177 to 25.5 ka (2σ ranges) and they are stratigraphically consistent. Only one age inversion is observed, which is shown by sample Dsz 6 (depth: 13.40 m). The post-IR OSL method again yields the youngest ages for Dsz 3 and Dsz 4, while the OSL and pIRIR@225 ages are overlapping within uncertainties for sample Dsz 4. It is believed that the lower part of the sequence can be interpreted based on both the pIRIR@225 and 290 ages. According to these data, formation of the paleosol complex at the base of the studied section (14.50-12.30 m, units 2-4) took place in an interval of ca. 130 to 70 ka corresponding to MIS 5e to 5a. This fossil soil complex (S1) can be correlated with the basal pedocomplex of the Süttő section in Hungary (Novothny et al., 2011), the V-S1 soil complex in the southern part of the Carpathian Basin (Vojvodina, Serbia) (Marković et al., 2011; Fitzsimmons et al., 2012), the upper well-developed soil horizon (F2, S3) in the Vukovar section in Croatia (Wacha and Frechen, 2011), and represents the Mende Upper 2 (MF2) soil according to the old Hungarian lithostratigraphic nomenclature (Pécsi 1995; Frechen et al., 1997; Horváth and Bradák, 2014; Újvári et al., 2014b). Pedogenesis has apparently been interrupted by loess sedimentation for a short period as revealed by the loess layer between depths of 12.95 and 12.60 m (unit 3). Accumulation of this loess layer captured by pIRIR@225 and 290 ages of 84.7±3.1 and 84.4±4.6 ka (Dsz 5) may be correlated with MIS 5b. The pIRIR@225 age from Dsz 4 (62.6±2.6 ka) suggest that this 1.30 m thick loess layer (12.30-11.00 m, unit 5) deposited during MIS 4. Weathered material between 11.00 and 8.30 m (unit 6; pIRIR@225 and 290 ages: 35.7±1.2 and 43.6±2.3 ka) that has visibly been affected by weak pedogenesis developed during the generally milder, wetter MIS 3 interval (van Andel, 2002), is correlated with V-L1S1 in Serbia (Marković et al., 2008; Buggle et al., 2009; Fitzsimmons et al., 2012).

5. Conclusions

Our dating framework that has been done on the Dunaszekcső loess-paleosol record demonstrates that some minute gastropods such as *S. oblonga* and *V. crystallina* reveal minor age anomalies and considerable overlaps in 2σ age ranges when compared with charcoal ^{14}C data and we conclude they yield reliable ^{14}C ages from loess. These species together with others from genera *Cochlicopa, Columella, Euconulus, Discus, Punctum, Nesovitrea*, etc. that have been shown to provide ages with no or only slight age anomalies (Pigati et al., 2010) can probably be used to create reliable age-depth models for loess sections spanning the last 40 ka. Calibrated ^{14}C ages from mollusc shells have an order of magnitude lower 2σ age error ranges than OSL/IRSL ages, further justifying their use in establishing precise chronologies within 40 ka. Obviously, these observations and assumptions deserve further testing in subsequent studies on the ^{14}C dating of loess molluscs.

OSL and IRSL ages (except for pIRIR@225) show discrepancies on the order of several thousands of years compared to ^{14}C ages and mostly have large scatters in ages. In such a case when two supposedly robust chronometers (^{14}C and OSL/IRSL) contradict each other it is hard to decide which is correct in lack of further independent age constraints. However, arguments such as consistent ^{14}C ages of charcoals and small molluscs, phases having very different origin and genesis, suggest that these ages are reliable and may reflect the real age of sedimentation. The sometimes significant discrepancies between ^{14}C and OSL/IRSL ages over the interval of 20-35 ka apparently exclude age modeling based on a mixture of ^{14}C and OSL/IRSL ages. Further, since the 2σ age ranges of the OSL/IRSL data are too large it is foreseen that their use in age-depth models for 10 to 40 ka will result in an unwanted broadening of age model uncertainties.

To address issues such as synchroneity and leads and lags between paleoenvironmental events across entire regions within 40 ka, both accurate and precise chronologies are needed that are based on numerous ^{14}C ages. For such purposes a dating resolution of 20 to 30 cm per dated sample is thought to be a minimum for loess profiles. However, further radiocarbon dates from above and below event horizons may be required to better constrain their timing, and also other stratigraphic markers like tephra horizons and geomagnetic excursions should be utilized in direct correlations and for improving age models.

As shown by the AMS radiocarbon and OSL/IRSL dates the upper ca. 15 m part of the Dunaszekcső loess sequence is an archive of paleoenvironmental changes of the last 130 ka with distinct periods of significant loess accumulations during the MIS 4 and MIS 3-2 (30 to 22 ka and beyond). The pedocomplex at the base of this section represent the last interglacial (Eemian, MIS 5e) and subsequent MIS 5 stages with one visible interruption of pedogenesis likely corresponding to MIS 5b. The generally milder and wetter MIS 3 left its imprint on the record by forming a 2.7 m thick, weakly weathered loess/soil horizon.

Acknowledgements

This work has been funded by post doc projects from the Hungarian Scientific Research Fund to GÚ (OTKA PD-108639) and to ÁN (OTKA PD-100315). Additional financial support provided by the Bolyai János Research Scholarship of the Hungarian Academy of Sciences (GÚ) and the EU through the TÁMOP-4.2.2.C-11/1/KONV–2012-0015 Earth System, the SROP-4.2.1.B-10/2/KONV-2010-0002 and ENVIKUT (TÁMOP-4.2.2.A-11/1/KONV-2012-0043) projects is gratefully acknowledged. Special thanks to Christine Thiel, Jan-Pieter Buylaert and Andrew Murray for the fruitful discussions on post-IR IRSL dating and for the possibility to etching fine-grained samples at the Nordic Laboratory for Luminescence Dating, Risø National Laboratory, Roskilde, Denmark. Guest editor Achim Brauer and the two anonymous referees are thanked for their valuable input which helped us to refine the original manuscript substantially.

References

Adamiec, G., Aitken, M. 1998. Dose rate conversion factors: update. Ancient TL 16, 37-50.

Alon, D., Mintz, G., Cohen, I., Weiner, S., Boaretto, E., 2002. The use of Raman spectroscopy to monitor the removal of humic substances from charcoal: quality control for ^{14}C dating of charcoal. Radiocarbon 44, 1–11.

Andersen, K.K., Svensson, A., Rasmussen, S.O., Steffensen, J.P., Johnsen, S.J., Bigler, M., Röthlisberger, R., Ruth, U., Siggaard-Andersen, M.-L., Dahl-Jensen, D., Vinther, B.M., Clausen, H.B., 2006. The Greenland ice core chronology 2005, 15–42 ka. Part 1: constructing the time scale. Quaternary Science Reviews 25, 3246–3257.

Antoine, P., Rousseau, D.D., Fuchs, M., Hatté, C., Gautier, C., Markovic, S.B., Jovanovic, M., Gaudenyi, T., Moine, O., Rossignol, J., 2009a. High resolution record of the last climatic cycle in the Southern Carpathian basin (Surduk, Vojvodina, Serbia). Quaternary International 198, 19–36.

Antoine, P., Rousseau, D. D., Moine, O., Kunesch, S., Hatté, C., Lang, A., Tissoux, H., and Zoeller, L., 2009b. Rapid and cyclic aeolian deposition during the Last Glacial in European loess: a high-resolution record from Nussloch, Germany, Quaternary Science Reviews 28, 2955–2973.

Ascough, P.L., Bird, M.I., Francis, S.M., Lebl, T., 2011. Alkali extraction of archaeological and geological charcoal: evidence for diagenetic degradation and formation of humic acids. Journal of Archaeological Science 38, 69–78.

Balakrishnan, M., Yapp, C.J., 2004. Flux balance models for the oxygen and carbon isotope compositions of land snail shells. Geochimica et Cosmochimica Acta 68, 2007–2024.

Barta, G., 2011. Secondary carbonates in loess-paleosoil sequences: a general review. Central European Journal of Geosciences 3, 129–146.

Becze-Deák, J., Langohr, R., Verrecchia, E., 1997. Small scale secondary $CaCO_3$ accumulations in selected sections of the European loess belt: morphological forms and potential for paleoenvironmental reconstruction. Geoderma 76, 221–252.

Bird, M.I., 2006. Radiocarbon dating of charcoal. In: Elias, S.A. (Ed.), The Encyclopaedia of Quaternary Science. Elsevier, Amsterdam, pp. 2950–2958.

Bird, M.I., Ascough, P.L., 2012. Isotopes in pyrogenic carbon: a review. Organic Geochemistry 42, 1529–1539.

Bird, M.I., Ayliffe, L.K., Fifield, K., Cresswell, R., Turney, C., 1999. Radiocarbon dating of 'old' charcoal using a wet oxidation e stepped combustion procedure. Radiocarbon 41, 127–140.

Bird, M.I., Fifield, L.K., Santos, G.M., Beaumont, P.B., Zhou, Y., di Tada, M.L., Hausladen, P.A., 2003. Radiocarbon dating from 40 to 60 ka BP at Border Cave, South Africa. Quaternary Science Reviews 22, 943–947.

Bird, I.M., Levchenko, V., Ascough, P.L., Meredith, W., Wurster, C.M., Williams, A., Tilston, E.L., Snape, C. E., Apperley, D.C., 2014. The efficiency of charcoal decontamination for radiocarbon dating by three pre-treatments e ABOX, ABA and hypy. Quaternary Geochronology 22, 25–32.

Blaauw, M., 2012. Out of tune: the dangers of aligning proxy archives. Quaternary Science Reviews 36, 38–49.

Blockley, S.P.E., Lane, C.S., Hardiman, M., Rasmussen, S. O., Seierstad, I.K., Steffensen, J.P., Svensson, A., Lotter, A.F., Turney, C.S.M., Bronk Ramsey, C., INTIMATE members,

2012. Synchronisation of palaeoenvironmental records over the last 60,000 years, and an extended INTIMATE event stratigraphy to 48,000 b2k. Quaternary Science Reviews 36, 2–10.

Bokhorst, M.P., Vandenberghe, J., Sümegi, P., Lanczont, M., Gerasimenko, N.P., Matviishina, Z.N., Marković, S.B., Frechen, M., 2011. Atmospheric circulation patterns in central and eastern Europe during the Weichselian Pleniglacial inferred from loess grain-size records. Quaternary International 234, 62–74.

Bond, G., Broecker, W., Johnsen, S., McManus, J., Labeyrie, L., Jouzel, J., Bonani, G., 1993. Correlations between climate records from North Atlantic sediments and Greenland ice. Nature 365, 143–147.

Braadbaart, F., Poole, I., van Brussel, A.A., 2009. Preservation potential of charcoal in alkaline environments: an experimental approach and implications for the archaeological record. Journal of Archaeological Science 36, 1672–1679.

Brennan, R., Quade, J., 1997. Reliable Late-Pleistocene stratigraphic ages and shorter groundwater travel times from ^{14}C in fossil snails from the southern Great Basin. Quaternary Research 47, 329–336.

Bronk Ramsey, C., 2009. Bayesian analysis of radiocarbon dates. Radiocarbon 51, 337–360.

Buggle, B., Hambach, U., Glaser, B., Gerasimenko, N., Marković, S., Glaser, I., Zöller, L., 2009. Stratigraphy, and spatial and temporal paleoclimatic trends in South-eastern/Eastern European loess-paleosol sequences. Quaternary International 196, 86–106.

Buylaert J.-P., Jain, M., Murray, A.S., Thomsen, K.J., Jain, M. 2009. Testing the potential of an elevated temperature IRSL signal from K-feldspar. Radiation Measurements 44, 560-565.

Buylaert J.-P., Jain, M., Murray, A.S., Thomsen, K.J., Thiel, C., Sohbati, R., 2012. A robust feldspar luminescence dating method for Middle and Late Pleistocene sediments. Boreas 41, 435-451.

Dansgaard, W., Johnsen, S.J., Clausen, H.B., Dahl-Jensen, D., Gundestrup, N.S., Hammer, C.U., Hvidberg, C.S., Steffensen, J.P., Sveinbjörnsdottir, A.E., Jouzel, J., Bond, G., 1993. Evidence for general instability of past climate from a 250 kyr ice-core record. Nature 364, 218–220.

Douka, K., Higham, T., Sinitsyn, A., 2010. The influence of pre-treatment chemistry on the radiocarbon dating of Campanian ignimbrite-aged charcoal from Kostenki 14 (Russia). Quat. Res. 73, 583–587.

Evin, J., Marechal, J., Pachiaudi, C., 1980. Conditions involved in dating terrestrial shells. Radiocarbon 22, 545–555.

Fitzsimmons, K.E., Hambach, U., in press. Loess accumulation during the last glacial maximum: Evidence from Urluia, southeastern Romania. Quaternary International, doi: 10.1016/j.quaint.2013.08.005.

Fitzsimmons, K.E., Markovic, S.B., Hambach, U., 2012. Pleistocene environmental dynamics recorded in the loess of the middle and lower Danube basin. Quaternary Science Reviews 41, 104–118.

Fitzsimmons, K.E., Hambach, U., Veres, D., Iovita, R., 2013. The Campanian Ignimbrite eruption: new data on volcanic ash dispersal and its potential impact on human evolution. PLoS ONE 8(6), e65839. doi:10.1371/journal.pone.0065839.

Frechen, M.A., Horváth, E., Gábris, Gy, 1997. Geochronology of middle and upper Pleistocene loess sections in Hungary. Quaternary Research 48, 291–312.

Galović, L., Frechen, M., Halamić, J., Durn, G., Romić, M., 2009. Loess chronostratigraphy in Eastern Croatia—a luminescence dating approach. Quaternary International 198, 85–97.

Gocke, M., Gulyás, S., Hambach, U., Jovanovic, M., Kovács, G., Markovic, S.B., Wiesenberg, G.L.B., 2014. Biopores and root features as new tools for improving paleoecological understanding of terrestrial sediment-paleosol sequences. Palaeogeography, Palaeoclimatology, Palaeoecology 394, 42–58.

Gocke, M., Kuzyakov, Y., Wiesenberg, G.L., 2010. Rhizoliths in loess—evidence for post-sedimentary incorporation of root-derived organic matter in terrestrial sediments as assessed from molecular proxies. Organic Geochemistry 41, 1198–1206.

Gocke, M., Pustovoytov, K., Kuhn, P., Wiesenberg, G., Löscher, M., Kuzyakov, Y., 2011. Carbonate rhizoliths in loess and their implications for paleoenvironmental reconstruction revealed by isotopic composition: $\delta^{13}C$, ^{14}C. Chemical Geology 283, 251–260.

Goodfriend, G.A., 1987. Radiocarbon age anomalies in shell carbonate of land snails from semi-arid areas. Radiocarbon 29, 159–167.

Goodfriend, G.A., Hood, D.G., 1983. Carbon isotope analysis of land snail shells: implications for carbon sources and radiocarbon dating. Radiocarbon 25, 810–830.

Goodfriend, G.A., Stipp, J.J., 1983. Limestone and the problem of radiocarbon dating of land-snail shell carbonate. Geology 11, 575–577.

Haesaerts, P., Borziac, I., Chekha, V.P., Chirica, V., Damblon, F., Drozdov, N.I., Orlova, L.A., Pirson, S., van der Plicht, J., 2009. Climatic signature and radiocarbon chronology of Middle and Late Pleniglacial loess from Eurasia: comparison with the Marine and Greenland records. Radiocarbon 51, 301–318.

Hatté, C., Pessenda, L.C.R., Lang, A., Paterne, M., 2001. Development of an accurate and reliable ^{14}C chronology for loess sequences: Application to the loess sequence of Nussloch (Rhine valley, Germany). Radiocarbon 43, 611–618.

Häggi, C., Zech, R., McIntyre, C., Eglinton, T., 2013. On the stratigraphic integrity of leaf-wax biomarkers in loess-paleosols. Biogeosciences Discussions 10, 16903–16922.

Higham, T., Brock, F., Peresani, M., Broglio, A., Wood, R., Douka, K., 2009. Problems with radiocarbon dating the Middle to upper Palaeolithic transition in Italy. Quaternary Science Reviews 28, 1257–1267.

Horváth, E., Bradák, B., 2014. Sárga föld, lősz, lösz: Short historical overview of loess research and lithostratigraphy in Hungary. Quaternary International 319, 1–10.

Huntley, D.J., Baril, M.R., 1997. The K content of the K-feldspars being measured in optical dating or in thermoluminescence dating. Ancient TL 15, 11–13.

Huntley, D.J., Lamothe, M., 2001. Ubiquity of anomalous fading in K-feldspars, and the measurement and correction for it in optical dating. Canadian Journal of Earth Sciences, 38, 1093-1106.

Johnsen, S.J., Clausen, H.B., Dansgaard, W., Fuhrer, K., Gundestrup, N., Hammer, C.U., Iversen, P., Jouzel, J., Stauffer, B., Steffensen, J.P., 1992. Irregular glacial interstadials recorded in a new Greenland ice core. Nature 359, 311–313.

Jull, A.J.T., Burr, G.S., Beck, J.W., Hodgins, G.W.L., Biddulph, D.L., Gann, J., Hatheway, A.L., Lange, T.E., Lifton, N.A., 2006. Application of accelerator mass spectrometry to environmental and paleoclimate studies at the University of Arizona. Radioactivity in the Environment 8, 3–23.

Kadereit, A., Kind, C-J., Wagner, G.A., 2013. The chronological position of the Lohne Soil in the Nussloch loess section — re-evaluation for a European loess-marker horizon. Quaternary Science Reviews 59, 67–86.

Klappa, C.F., 1980. Rhizoliths in terrestrial carbonates: classification, recognition, genesis and significance. Sedimentology 27, 613–629.

Lang, A., Hatté, C., Rousseau, D.-D., Antoine, P., Fontugne, M., Zöller, L., Hambach, U., 2003. High-resolution chronologies for loess: comparing AMS ^{14}C and optical dating results. Quaternary Science Reviews, Quaternary Geochonology 22, 953–959.

Lian, O.B., Roberts, R.G., 2006. Dating the Quaternary: progress in luminescence dating of sediments. Quaternary Science Reviews 25, 2449–2468.

Lowe, J.J., Rasmussen, S.O., Bjorck, S., Hoek, W.Z., Steffensen, J.P., Walker, M.J.C., Yu, Z.C., 2008. Synchronisation of palaeoenvironmental events in the North Atlantic region during the Last Termination: a revised protocol recommended by the INTIMATE group. Quaternary Science Reviews 27, 6–17.

Marković, S.B., Bokhorst, M., Vandenberghe, J., Oches, E.A., Zöller, L., McCoy, W.D., Gaudenyi, T., Jovanovic, M., Hambach, U., Machalett, B., 2008. Late Pleistocene loess-paleosol sequences in the Vojvodina region, North Serbia. Journal of Quaternary Science 23, 73–84.

Marković, S.B., Hambach, U., Stevens, T., Kukla, G.J., Heller, F., McCoy, W.D., Oches, E.A., Buggle, B., Zöller, L., 2011. The last million years recorded at the Stari Slankamen (Northern Serbia) loess-palaeosol sequence: revised chronostratigraphy and long-term environmental trends. Quaternary Science Reviews 30, 1142–1154.

McGeehin, J.P., Burr, G.S., Jull, A.J.T., Reines, D., Gosse, J., Davis, P.T., Muhs, D., Southon, J.R., 2001. Stepped-combustion ^{14}C dating of sediment: a comparison with established techniques. Radiocarbon 43, 255–261.

Moine, O., Rousseau, D.-D., Antoine, P., 2008. The impact of Dansgaard-Oeschger cycles on the loessic environment and malacofauna of Nussloch (Germany) during the upper Weichselian. Quaternary Research 70, 91–104.

Molnár, M., Janovics, R., Major, I., Orsovszki, J., Gönczi, R., Veres, M., Leonard, A.G., Castle, S.M., Lange, T.E., Wacker, L., Hajdas, I., Jull, A.J.T., 2013a. Status report of the new AMS 14C sample preparation lab of the Hertelendy Laboratory of Environmental Studies (Debrecen, Hungary). Radiocarbon 55, 665–676.

Molnár, M., Rinyu, L., Veres, M., Seiler, M., Wacker, L., Synal, H-A., 2013b. ENVIRONMICADAS: a mini 14C AMS with enhanced gas ion source interface in the Hertelendi Laboratory of Environmental Studies (HEKAL), Hungary. Radiocarbon 55, 338–344.

Murray, A.S., Wintle, A.G. 2000. Luminescence dating of quartz using an improved regenerative-dose protocol. Radiation Measurements 32, 57–73.

Murray, A.S., Wintle, A.G. 2003. The single aliquot regenerative dose protocol: potential for improvements in reliability. Radiation Measurements 37, 377-381.

Murray, A.S., Schmidt, E.D., Stevens, T., Buylaert, J.-P., Marković, S.B., Tsukamoto, S., Frechen. 2014. Dating Middle Pleistocene loess from Stari Slankamen (Vojvodina, Serbia) – Limitations imposed by the saturation behaviour of an elevated temperature IRSL signal. Catena 117, 34-42.

Murray, A.S., Thomsen, K.J., Masuda, N., Buylaert, J.P., Jain, M., 2012. Identifying well-bleached quartz using the different bleaching rates of quartz and feldspar luminescence signals. Radiation Measurements 47, 688–695.

Novothny, Á., Horváth, E., Frechen, M., 2002. The loess profile at Albertirsa, Hungary–improvements in loess stratigraphy by luminescence dating. Quaternary International 95–96, 155–163.

Novothny, Á., Frechen, M., Horváth, E., Bradák, B., Oches, E.A., McCoy, W., Stevens, T., 2009. Luminescence and amino acid racemization chronology and magnetic susceptibility record of the loess e paleosol sequence at Süttő, Hungary. Quaternary International 198, 62–76.

Novothny, Á., Frechen, M., Horváth, E., Wacha, L., Rolf, C., 2011. Investigating the penultimate and last glacial cycles of the Süttő loess section (Hungary) using luminescence dating, high-resolution grain size, and magnetic susceptibility data. Quaternary International 234, 75–85.

Pécsi, M., 1995. Loess stratigraphy and Quaternary climatic change. In: Pécsi, M., Schweitzer, F. (Eds.), Concept of Loess, Loess-paleosol Stratigraphy. Loess in Form, vol. 3, pp. 23–30.

Pigati, J.S., McGeehin, J.P., Muhs, D.R., Bettis III, E.A., 2013. Radiocarbon dating late Quaternary loess deposits using small terrestrial gastropod shells. Quaternary Science Reviews 76, 114–128.

Pigati, J.S., Quade, J., Shanahan, T.M., Haynes Jr., C.V., 2004. Radiocarbon dating of minute gastropods and new constraints on the timing of spring-discharge deposits in southern Arizona, USA. Palaeogeography, Palaeoclimatology, Palaeoecology 204, 33–45.

Pigati, J.S., Rech, J.A., Nekola, J.C., 2010. Radiocarbon dating of small terrestrial gastropod shells in North America. Quaternary Geochronology 5, 519–532.

Porter, S. C., An, Z. S., 1995. Correlation between climate events in the North Atlantic and China during the last glaciation, Nature 375, 305–308.

Prescott, J.R., Hutton, J. T. 1994. Cosmic ray contribution to dose rates for luminescence and ESR dating: large depth and long-term time variations. Radiation Measurements 23, 497-500.

Preston, C.M., Schmidt, M.W.I., 2006. Black, pyrogenic carbon: a synthesis of current knowledge and uncertainties with special consideration of boreal regions. Biogeosciences 3, 397–420.

Procków, M., 2009. The genus Trochulus Chemnitz, 1786 (Gastropoda: Pulmonata: Hygromiidae) – a taxonomic revision. Folia Malacologica 17, 101–176.

Pustovoytov, K., Terhorst, B., 2004. An isotopic study of a late Quaternary loess–paleosol sequence in SW Germany. Revista Mexicana de Ciencias Geologicas 21, 88–93.

Pye, K., 1983. Grain surface textures and carbonate content of late Pleistocene loess from West Germany and Poland. Journal of Sedimentary Petrology 53, 973–980.

Pye, K., 1995. Nature, origin and accumulation of loess. Quaternary Science Reviews 14, 653–667.

Rasmussen, S.O., Andersen, K.K., Svensson, A.M., Steffensen, J.P., Vinther, B.M., Clausen, H.B., Siggaard-Andersen, M.-L., Johnsen, S.J., Larsen, L.B., Dahl-Jensen, D., Bigler, M., Röthlisberger, R., Fischer, H., Goto-Azuma, K., Hansson, M.E., Ruth, U., 2006. A new Greenland ice core chronology for the last glacial termination. Journal of Geophysical Research 111, D6.

Rebollo, N.R., Cohen-Ofri, I., Popovitz-Biro, R., Bar-Yosef, O., Meignen, L., Goldberg, P., Weiner, S., Boaretto, E., 2008. Structural characterisation of charcoal exposed to high and low pH; implications for ^{14}C sample preparation and charcoal preservation. Radiocarbon 50, 289–307.

Rees-Jones, J., 1995. Optical dating of young sediments using fine-grain quartz. Ancient TL 13, 9-14 .

Reimer, P.J., Bard,E., Bayliss, A., Warren Beck, J., Blackwell, P.G., Bronk Ramsey, Ch., Grootes, P.M., Guilderson, T.P., Haflidason, H., Hajdas, I., Hatté, Ch., Heaton, T.J., Hoffmann, D.L., Hogg, A.G., Hughen, K.A., Kaiser, K.F., Kromer, B., Manning, S.W., Niu, M., Reimer, R.W., Richards, D.A., Scott, E.M., Southon, J.R., Staff, R.A., Turney, Ch.S.M., van der Plicht, J., 2013. IntCal13 and Marine13 radiocarbon age calibration curves 0-50,000 years cal BP. Radiocarbon 55, 1869–1887.

Rolf, C., Hambach, U., Novothny, Á., Horváth, E., Schnepp, E., 2014. Dating of a Last Glacial loess sequence by relative geomagnetic palaeointensity: A case study from the Middle Danube Basin (Süttő, Hungary). Quaternary International 319, 99–108.

Rousseau, D. D., Antoine, P., Hatté, C., Lang, A., Zoeller, L., Fontugne, M., Ben Othman, D., Luck, J. M., Moine, O., Labonne, M., Bentaleb, I., Jolly, D., 2002. Abrupt millennial climatic changes from Nussloch (Germany) Upper Weichselian eolian records during the Last Glaciation, Quaternary Science Reviews 21, 1577–1582.

Rousseau, D. D., Sima, A., Antoine, P., Hatté, C., Lang, A., Zoeller, L., 2007. Link between European and North Atlantic abrupt climate changes over the last glaciation, Geophysical Research Letters 34, L22713, doi:10.1029/2007gl031716.

Rubin, M., Likins, R.C., Berry, E.G., 1963. On the validity of radiocarbon dates from snail shells. Journal of Geology 71, 84–89.

Schatz, A-K., Buylaert, J-P., Murray, A.S., Stevens, T., Scholten, T. 2012. Establishing a luminescence chronology for a palaeosol-loess profile at Tokaj (Hungary): A comparison of quartz OSL and polymineral IRSL signals. Quaternary Geochronology 10, 68-74.

Schmidt, E.D., Frechen, M., Murray, A.S., Tsukamoto, S., Bittmann, F., 2011. Luminescence chronology of the loess record from the Tönchesberg section: A comparison of using quartz and feldspar as dosimeter to extend the age range beyond the Eemian. Quaternary International 234, 10–22.

Schmidt, E.D., Machalett, B., Markovic, S.B., Tsukamoto, S., Frechen, M., 2010. Luminescence chronology of the upper part of the Stari Slankamen loess sequence (Vojvodina, Serbia). Quaternary Geochronology 5, 137–142.

Shi, C., Zhu, R., Glass, B.P., Liu, Q., Zema, A., Suchy, V. 2003. Climate variations since the last interglacial recorded in Czech loess. Geophysical Research Letters, 30 (11), 1562.

Stevens, T., Armitage, S.J., Lu, H., Thomas, D.S.G., 2006. Sedimentation and diagenesis of Chinese loess: Implications for the preservation of continuous high-resolution climate records. Geology 34, 849–852.

Stevens, T., Lu, H., Thomas, D.S.G., Armitage, S.J., 2008. Optical dating of abrupt shifts in the late Pleistocene East Asian monsoon. Geology 36, 415–418.

Stevens, T., Marković, S.B., Zech, M., Hambach, U., Sümegi, P., 2011. Dust deposition and climate in the Carpathian Basin over an independently dated last glacial–interglacial cycle. Quaternary Science Reviews 30, 662–681.

Stevens, T., Thomas, D.S.G., Armitage, S.J., Lunn, H.R., and Lu, H., 2007. Reinterpreting climate proxy records from late Quaternary Chinese loess: A detailed OSL investigation. Earth-Science Reviews 80, 111–136.

Sun, Y., Clemens, S.C., Morrill, C., Lin, X., Wang, X., An, Z., 2012. Influence of Atlantic meridional overturning circulation on the East Asian winter monsoon. Nature Geoscience 5, 46–49.

Sümegi, P., Hertelendi, E., 1998. Reconstruction of microenvironmental changes in the Kopasz Hill loess area at Tokaj (Hungary) between 15 and 70 ka BP. Radiocarbon 40, 855–863.

Sümegi P., Krolopp E., 2002. Quartermalacological analyses for modelling of the Upper Weichselian paleoenvironmental changes in the Carpathian basin. Quaternary International 91, 53–63.

Svensson, A., Andersen, K.K., Bigler, M., Clausen, H.B., Dahl-Jensen, D., Davies, S.M., Johnsen, S.J., Muscheler, R., Parrenin, F., Rasmussen, S.O., Röthlisberger, R., Seierstad, I.K., Steffensen, J.P., Vinther, B.M., 2008. A 60000 year Greenland stratigraphic ice core chronology. Climate of the Past 4, 47–57.

Synal, H-A., Stocker, M., Suter, M., 2007. MICADAS: a new compact radiocarbon AMS system. Nuclear Instruments and Methods in Physics Research B 259, 7–13.

Tamers, M.A., 1970. Validity of radiocarbon dates on terrestrial snail shells. American Antiquity 35, 94–100.

Telford, R.J., Heegaard, E., Birks, H.J.B., 2004. All age–depth models are wrong: but how badly? Quaternary Science Reviews 23, 1–5.

Thiel, C., Buylaert, J.-P., Murray, A., Terhorst, B., Hofer, I., Tsukamoto, S., Frechen, M., 2011. Luminescence dating of the Stratzing loess profile (Austria) - Testing the potential of an elevated temperature post-IR IRSL protocol. Quaternary International 234, 23–31.

Thiel, C., Horváth, M., Frechen, M., 2014. Revisiting the loess/palaeosol sequence in Paks, Hungary: A post-IR IRSL based chronology for the 'Younger Loess Series'. Quaternary International 319, 88–98.

Thomsen, K.J., Murray, A.S., Jain, M., Bøtter-Jensen, L., 2008. Laboratory fading rates of various luminescence signals from feldspar-rich sediment extracts. Radiation Measurements 43, 1474–1486.

Timar-Gabor, A., Wintle, A.G., 2013. On natural and laboratory generated dose response curves for quartz of different grain sizes from Romanian loess. Quaternary Geochronology 18, 34–40.

Tissoux, H., Valladas, H., Voinchet, P., Reyss, J.L., Mercier, N., Falguères, C., Bahain, J.-J., Zöller, L., Antoine, P., 2010. OSL and ESR studies of Aeolian quartz from the Upper Pleistocene loess sequence of Nussloch (Germany). Quaternary Geochronology 5, 131–136.

Trumbore, S.E., 2000. Radiocarbon geochronology. In: Noller, J.S., Sowers, J.M., Lettis, W.R. (Eds.), Quaternary Geochronology: Methods and Applications. American Geophysical Union, Washington, D.C, pp. 41–60.

Turney, C.S.M., Bird, M.I., Fifield, L.K., Roberts, R.G., Smith, M., Dortch, C.E., Grün, R., Lawson, E., Ayliffe, L.K., Miller, G.H., Dortch, J., Cresswell, R.G., 2001. Early human occupation at Devil's Lair, southwestern Australia 50,000 years ago. Quaternary Research 55, 3–13.

Újvári, G., Varga, A., Balogh-Brunstad, Z., 2008. Origin, weathering, and geochemical composition of loess in southwestern Hungary. Quaternary Research 69, 421–437.

Újvári, G., Mentes, Gy., Bányai, L., Kraft, J., Gyimóthy, A., Kovács, J., 2009. Evolution of a bank failure along the River Danube at Dunaszekcső, Hungary. Geomorphology 109, 197–209.

Újvári, G., Varga, A., Ramos, F.C., Kovács, J., Németh, T., Stevens, T., 2012. Evaluating the use of clay mineralogy, Sr e Nd isotopes and zircon U–Pb ages in tracking dust provenance: an example from loess of the Carpathian Basin. Chemical Geology 304–305, 83–96.

Újvári, G., Molnár, M., Novothny, Á., Kovács, J., 2014a. Establishing chronologies for loess records within 40 ka by AMS ^{14}C-dating of small mollusc shells. Geophysical Research Abstracts 16, EGU2014-4950-1.

Újvári, G., Varga, A., Raucsik, B., Kovács, J., 2014b. The Paks loess-paleosol sequence: A record of chemical weathering and provenance for the last 800 ka in the mid-Carpathian Basin. Quaternary International 319, 22–37.

van Andel, T.H., 2002. The Climate and Landscape of the Middle Part of the Weichselian Glaciation in Europe: The Stage 3 Project. Quaternary Research 57, 2–8.

Vandenberghe, J., Markovic, S.B., Jovanovic, M., Hambach, U., in press. Site-specific variability of loess and palaeosols (Ruma, Vojvodina, northern Serbia). Quaternary International, doi: 10.1016/j.quaint.2013.10.036.

Vandenberghe, J., Nugteren, G., 2001. Rapid climatic changes recorded in loess successions. Global and Planetary Change 28, 1–9.

Vasiliniuc, S., Timar-Gabor, A., Vandenberghe, D.A.G., Panaiotu, C.G., Begy, R.Cs., Cosma, C., 2011. A high resolution optical dating study of the Mostis¸ tea loess-palaeosol sequence (SE Romania) using sand-sized quartz. Geochronometria 38, 34–41.

Veres, D., Lane, C.S., Timar-Gabor, A., Hambach, U., Constantin, D., Szakács, A., Fülling, A., Onac, B.P., 2013. The Campanian Ignimbrite/Y5 tephra layer - A regional stratigraphic marker for isotope Stage 3 deposits in the Lower Danube region, Romania. Quaternary International 293, 22–33.

Wacha, L., Frechen, M., 2011. The geochronology of the "Gorjanović loess section" in Vukovar, Croatia. Quaternary International 240, 87–99.

Wacker, L., Bonani, G., Friedrich, M., Hajdas, I., Kromer, B., Némec, M., Ruff, M., Suter, M., Synal, H.A., Vockenhuber, C., 2010. MICADAS: Routine and high-precision radiocarbon dating. Radiocarbon 52, 252–262.

Wallinga, J., Murray, A.S., Duller, G.A.T., Tornqvist, T.E., 2001. Testing optically stimulated luminescence dating of sand-sized quartz and feldspar from fluvial deposits. Earth and Planetary Science Letters 193, 617–630.

Welter-Schultes, F.W., 2012. European non-marine molluscs, a guide for species identification. Planet Poster Editions, Göttingen, ISBN-13: 9783933922755, p. 757.

Wild, E.M., Steier, P., Fischer, P., Höflmayer, F., 2013. ^{14}C dating of humic acids from Bronze and Iron Age plant remains from the eastern Mediterranean. Radiocarbon 55, 599–607.

Winkler, S., Matthews, J.A. , 2010. Holocene glacier chronologies: are 'high-resolution' global and inter-hemispheric comparisons possible? The Holocene 20, 1137–1147.

Wintle, A.G. 1973. Anomalous fading of thermoluminescence in mineral samples, Nature 245, 143–144.

Wintle, A.G., 2008. Luminescence dating: where it has been and where it is going. Boreas 37, 471–482.

Wintle, A.G., Murray, A.S. 2006. A review of quartz optically stimulated luminescence characteristics and their relevance in single-aliquot regeneration dating protocols. Radiation Measurements 41, 369-391.

Wood, R.E., Douka, K., Boscato, P., Haesaerts, P., Sinitsyn, A., Higham, T.F.G., 2012. Testing the ABOx-SC method: dating known age charcoals associated with the Campanian Ignimbrite. Quaternary Geochronology 9, 16–26.

Xiao, J.L., Porter, S.C., An, Z.S., Kumai, H., Yoshikawa, S., 1995. Grain size of Quartz as an indicator of winter monsoon strength on the Chinese Loess Plateau of central China during the last 130, 000 yr. Quaternary Research 43, 22–29.

Xu, B., Gu, Z., Han, J., Hao, Q., Lu, Y., Wang, L., Wu, N., Peng, Y., 2011. Radiocarbon age anomalies of land snail shells in the Chinese Loess Plateau. Quaternary Geochronology 6, 383–389.

Yates, T., 1986. Studies of non-marine mollusks for the selection of shell samples for radiocarbon dating. Radiocarbon 28, 457–463.

Zhou, W., Head, W.J., Wang, F., Donahue, D.J., Jull, A.J.T., 1999. The reliability of AMS radiocarbon dating of shells from China. Radiocarbon 41, 17–24.

Figures and captions

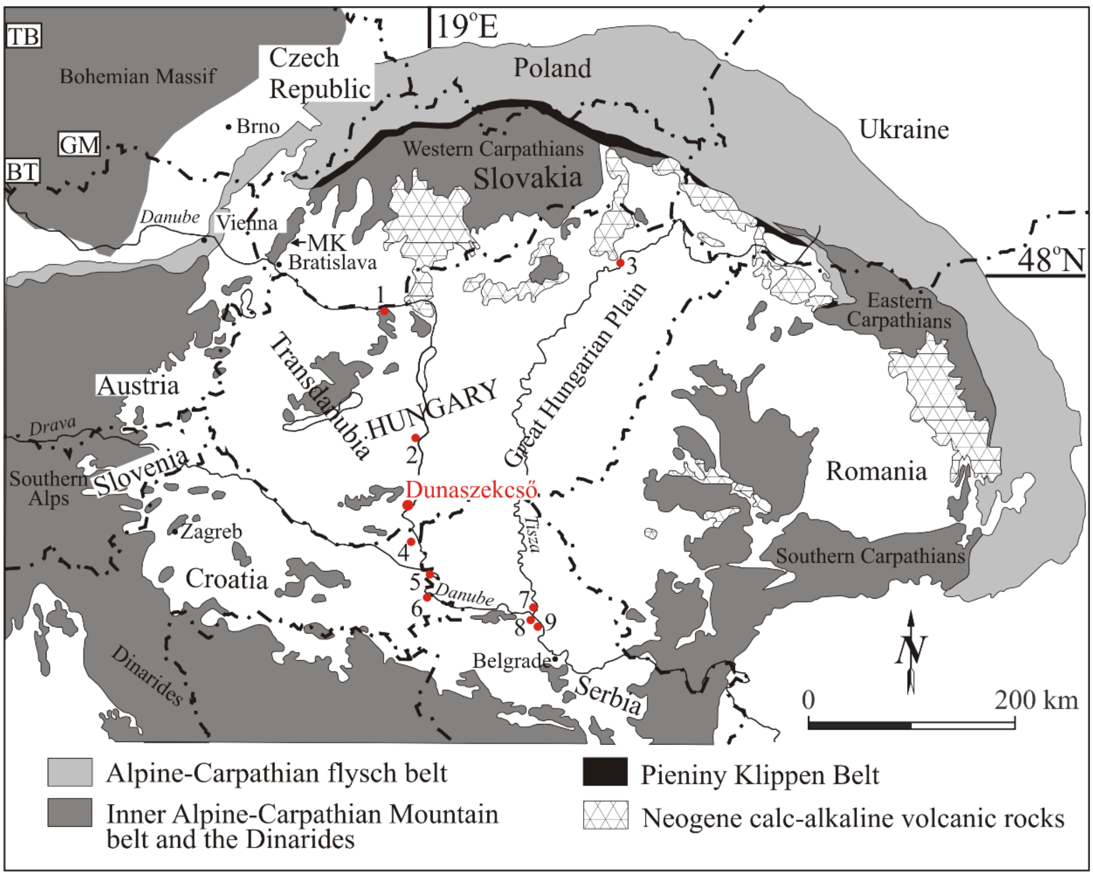

Figure 1. Locations of the Dunaszekcső loess sequence and other loess profiles in the Carpathian Basin mentioned in the text. 1. Süttő, 2. Paks, 3. Tokaj, 4. Zmajevac, 5. Erdut, 6. Vukovar, 7. Titel, 8. Stari Slankamen, 9. Surduk.

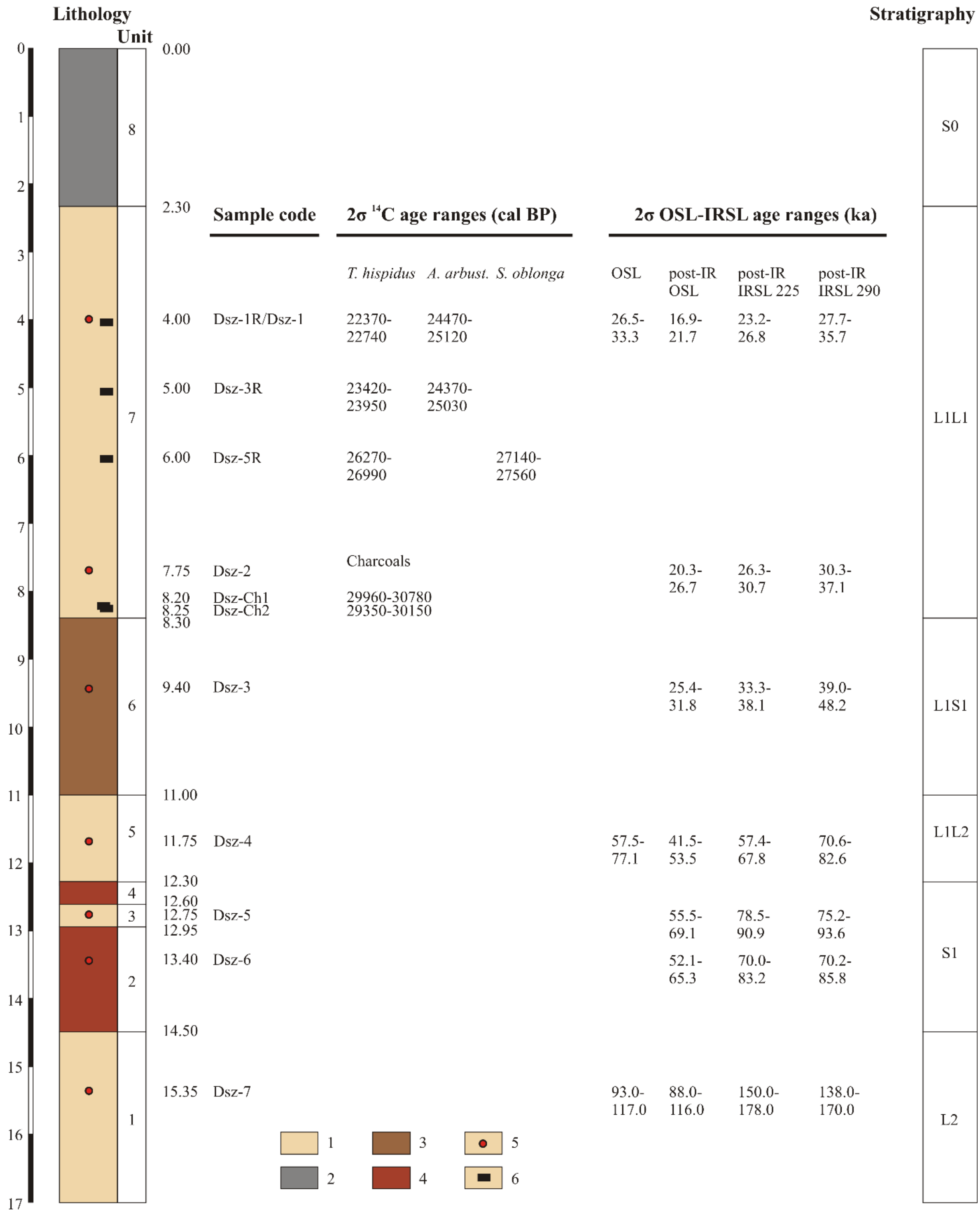

Figure 2. Stratigraphic log of the sampled profile exposed at Dunaszekcső and AMS radiocarbon (mollusc shells, charcoals) and OSL/IRSL age ranges. Legend: 1. loess, 2. recent (Holocene) soil, 3. weakly weathered soil horizon, 4. red-brown, well-developed pedocomplex, 5. position of OSL-IRSL sampling points, 6. position of loess cuboids cut for AMS radiocarbon

dating. Abbreviations: *T. hispidus* = *Trochulus hispidus, A. arbust.* = *Arianta arbustorum, S. oblonga* = *Succinella oblonga*.

Figure 3. Upper part of the studied loess profile and different phases subjected to AMS ^{14}C analyses. a) the loess profile with sampling points for grain size analyses and radiocarbon dating, b) and c) rhizoliths (hypocoatings), d) *Succinella oblonga*, e) *Vitrea crystallina*, f) Clausiliidae sp., g) *Trochulus hispidus*, h) charcoal fragments.

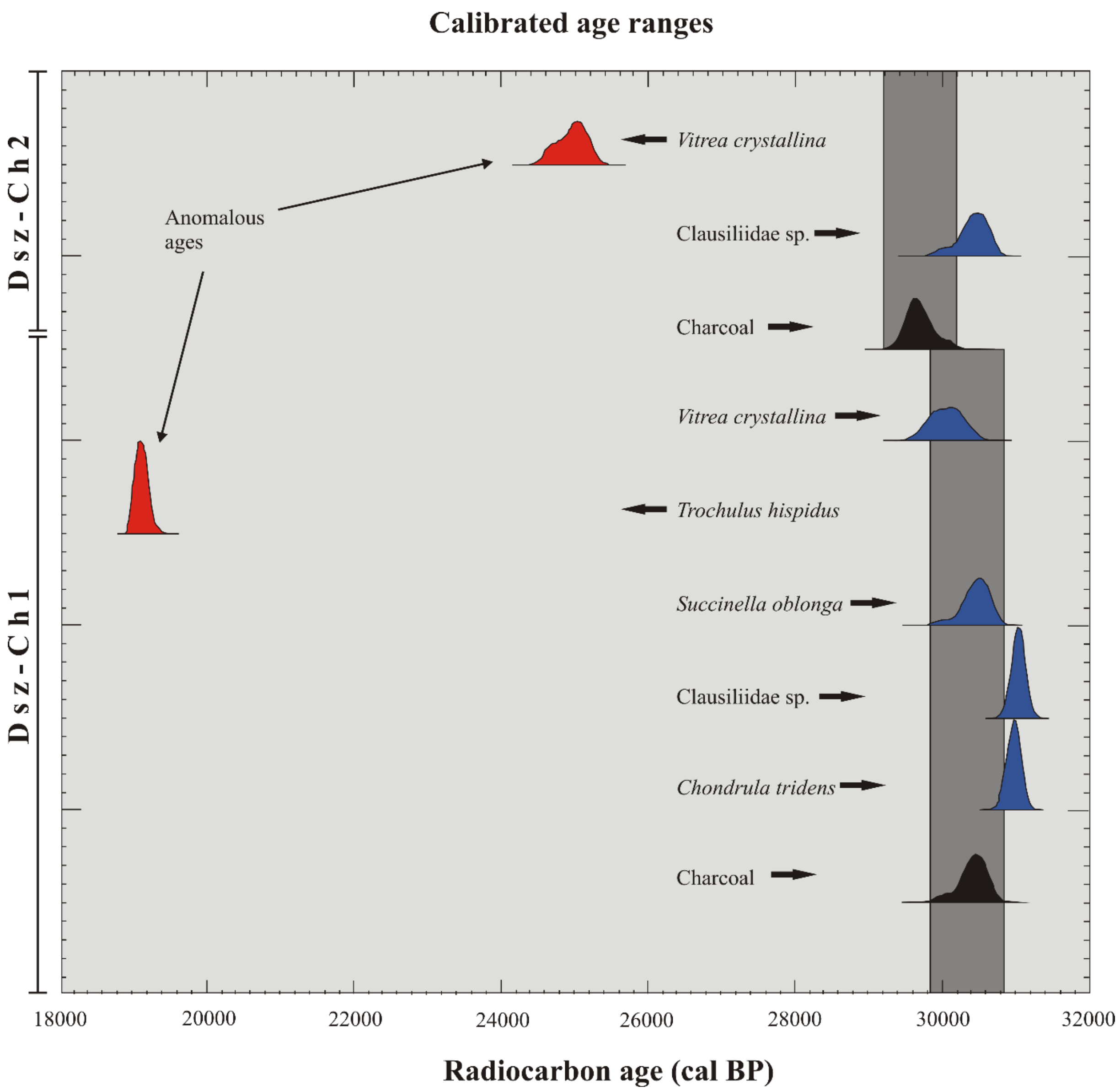

Figure 4. Comparison of calibrated radiocarbon age ranges of charcoal fragments and mollusc shells from samples Dsz-Ch1 and 2.

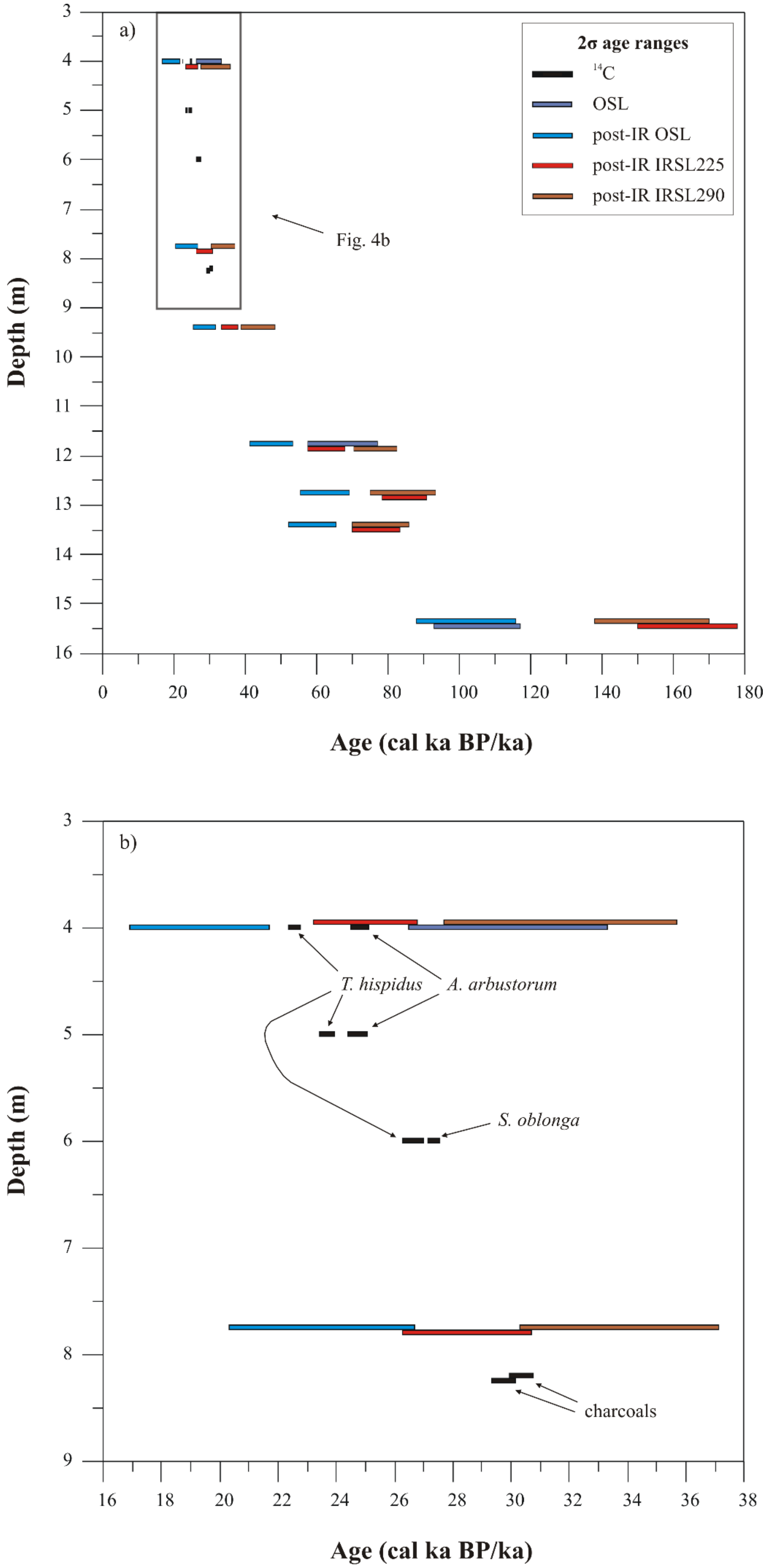

a)
2σ age ranges
14C
OSL
post-IR OSL
post-IR IRSL225
post-IR IRSL290
Fig. 4b
Depth (m)
Age (cal ka BP/ka)
b)
T. hispidus
A. arbustorum
S. oblonga
charcoals
Depth (m)
Age (cal ka BP/ka)

Figure 5. Radiocarbon (mollusc shell, charcoal) and OSL/IRSL age ranges (2σ) as a function of depth. Abbreviations: *A. arbustorum* = *Arianta arbustorum, S. oblonga* = *Succinella oblonga, T. hispidus* = *Trochulus hispidus*.

Supplementary material

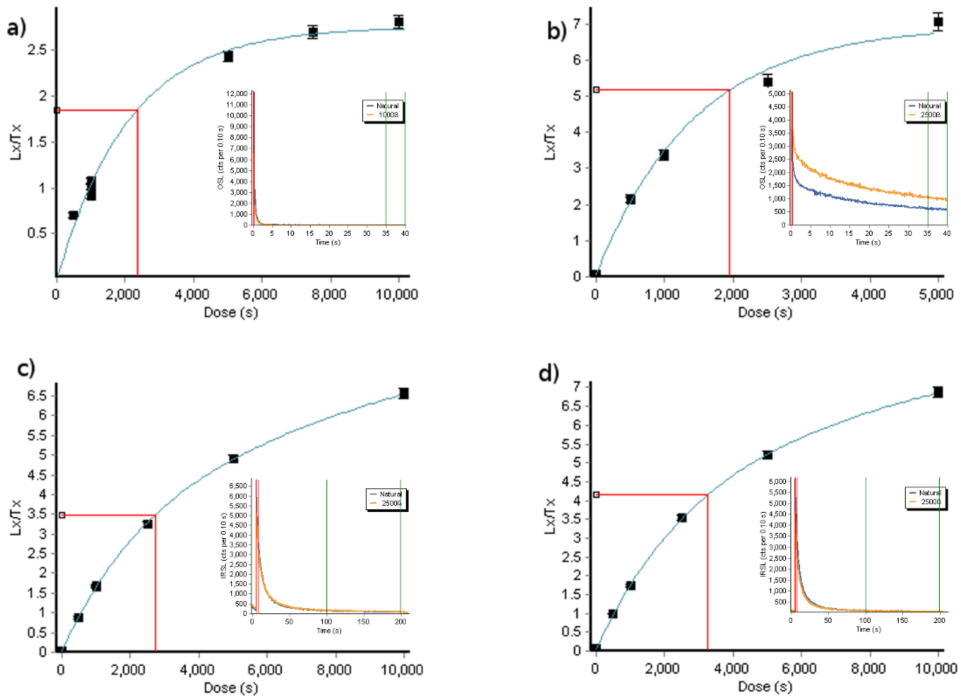

Figure S1. Dose-response and decay curves for a) quartz OSL, b) polymineral post-IR OSL, c) polymineral post-IR IRSL225 and d) polymineral post-IR IRSL290 signals from sample Dsz 4.

Tables

Table 1. AMS radiocarbon ages of mollusc shells, charcoals and rhizoltihs from the Dunaszekcső loess section

Sample depth (m)	Sample code	Dated material	Lab code	^{14}C age (yr BP)	±1σ	Calibrated 2σ age range (cal BP, 95.4% prob.)		Age anomaly (^{14}C yr)[b]	±1σ[c]
						Min	Max		
4.00	Dsz-1R	mollusc shell (A. arb.)	DeA-2067	20585	75	24470	25120		
	Dsz-1R	mollusc shell (T. hisp.)	DeA-2068	18678	68	22370	22740		
	Dsz-1R	rhizolith	DeA-2069	8846	36	9470	10160		
5.00	Dsz-3R	mollusc shell (A. arb.)	DeA-2070	20504	79	24370	25030		
	Dsz-3R	mollusc shell (T. hisp.)	DeA-2071	19656	76	23420	23950		
	Dsz-3R	rhizolith	DeA-2072	7269	33	8010	8170		
6.00	Dsz-5R	mollusc shell (S. obl.)	DeA-2931	23036	88	27140	27560		
	Dsz-5R	mollusc shell (T. hisp.)	DeA-2930	22332	80	26270	26990		
	Dsz-5R	rhizolith	DeA-2929	8639	42	9530	9690		
8.20	Dsz-Ch1	charcoal	DeA-2917	26101	110	29960	30780		
	Dsz-Ch1	mollusc shell (Ch. trid.)	DeA-2921	26851	118	30780	31170	750	161
	Dsz-Ch1	mollusc shell (Clausil. sp.)	DeA-2920	26979	126	30840	31240	878	167
	Dsz-Ch1	mollusc shell (S. obl.)	DeA-2919	26142	125	29990	30830	41	167
	Dsz-Ch1	mollusc shell (T. hisp.)	DeA-2918	15844	56	18920	19290	-10257	123
	Dsz-Ch1	mollusc shell (V. cryst.)	DeA-2922	25838	123	29600	30530	-263	165
8.25	Dsz-Ch2	charcoal	DeA-2923	25568	105	29350	30150		
	Dsz-Ch2	mollusc shell (Clausil. sp.)	DeA-2925	26113	129	29930	30800	545	166
	Dsz-Ch2	mollusc shell (V. cryst.)[a]	DeA-2924	20724	111	24540	25320	-4844	153

Conventional ^{14}C ages have been calibrated using OxCal 4.2 Online and the IntCal13 calibration curve.
Abbreviations: A. arb. = *Arianta arbustorum* (Linnaeus, 1758), Ch. trid. = *Chondrula tridens* (Müller, 1774), Clausil. sp. = Clausiliidae sp. indet. , S. obl. = *Succinella oblonga* (Draparnaud, 1801), T. hisp. = *Trochulus hispidus* (Linneaus, 1758), V. cryst. = *Vitrea crystallina* (Müller, 1774).

[a]Low current in AMS and problems with the background correction due to very small sample size (0.2 mg C), leading to younger ages.

[b]Age anomalies are calculated as conventional ^{14}C age$_{shell}$-^{14}C age$_{charcoal}$, against the charcoal in the respective sample. Positive deviations indicate that the shell ages are too old.

[c]Uncertainties of age anomalies are calculated from the conventional ^{14}C age errors (1σ) as $\sigma_A = (\sigma_{charcoal}^2+\sigma_{shell}^2)^{1/2}$

Table 2. Gamma spectrometry results for loess and paleosol samples of the Dunaszekcső section

Sample code	Activity concentrations (Bq kg^{-1})												Element concentrations (ppm)				Specific activity (Bq kg^{-1})	Radioactive equilibrium (Ra U^{-1})
	^{235}U	^{234}Th	^{226}Ra	^{214}Pb	^{214}Bi	^{210}Pb	^{228}Ac	^{212}Pb	^{212}Bi	^{208}Tl	^{40}K	^{137}Cs	U	Ra Ue[a]	Th	K		
Dsz-1	1.6	37	37	36	37	54	40	44	40	40	450	<1	3.01	3.01	10.25	15000	101	1.0
Dsz-2	1.7	39	39	37	37	53	44	44	44	44	500	<1	3.17	3.17	11.00	16667	108	1.0
Dsz-3	1.8	40	40	39	39	49	46	46	46	46	566	<1	3.25	3.25	11.50	18867	116	1.0
Dsz-4	1.7	38	34	32	32	37	39	39	40	39	430	<1	3.09	2.76	9.81	14333	98	0.9
Dsz-5	1.5	34	34	34	33	50	40	40	40	40	475	<1	2.76	2.76	10.00	15833	103	1.0
Dsz-6	2.1	48	40	40	40	60	50	50	48	52	540	<1	3.90	3.25	12.50	18000	120	0.8
Dsz-7	1.5	33	33	30	30	45	40	40	38	38	400	<1	2.68	2.68	9.75	13333	94	1.0

[a]Uranium equivalent radium concentration, i.e. U concentration that is in radioactive equilibrium with Ra measured in the sample.

Table 3. Dose rate, equivalent dose (D_e) and OSL/post-IR OSL ages

Sample depth (m)	Sample code	Water content (%)	Dose rate [Gy/ka]		Quartz D_e [Gy]				Quartz ages [ka]			
			OSL	post-IR OSL	OSL	n	post-IR OSL	n	OSL age	1σ	post-IR OSL age	1σ
4.00	Dsz-1	15±5	2.91±0.17	3.10±0.17	86.81±0.47	12	59.77±1.75	3	29.9	1.7	19.3	1.2
7.75	Dsz-2	15±5		3.30±0.18			77.56±3.07	8			23.5	1.6
9.40	Dsz-3	15±5		3.54±0.18			101.27±2.03	8			28.6	1.6
11.75	Dsz-4	15±5	2.76±0.17	2.95±0.17	186.16±7.22	12	140.33±3.53	3	67.3	4.9	47.5	3.0
12.75	Dsz-5	20±5		2.85±0.15			177.65±2.60	3			62.3	3.4
13.40	Dsz-6	20±5		3.52±0.19			206.80±3.21	3			58.7	3.3
15.35	Dsz-7	20±5	2.44±0.15	2.60±0.15	254.40±3.08	11	263.81±12.14	3	105.0	6.0	102.0	7.0

n = number of aliquots used for equivalent dose estimation

Table 4. Dose rate, equivalent dose (D_e) and post-IR IRSL ages

Sample depth (m)	Sample code	Water content (%)	Dose rate for post-IR IRSL [Gy/ka]	Feldspar D_e [Gy]				Feldspar ages [ka]			
				post-IR IRSL 225	n	post-IR IRSL 290	n	post-IR IRSL 225 age	1σ	post-IR IRSL 290 age	1σ
4.00	Dsz-1	15±5	3.29±0.12	82.31±0.15	9	104.17±5.40	9	25.0	0.9	31.7	2.0
7.75	Dsz-2	15±5	3.50±0.13	99.92±1.60	9	118.02±4.22	9	28.5	1.1	33.7	1.7
9.40	Dsz-3	15±5	3.75±0.13	133.76±0.94	9	163.47±6.34	9	35.7	1.2	43.6	2.3
11.75	Dsz-4	15±5	3.14±0.12	196.69±3.39	9	240.87±1.70	9	62.6	2.6	76.6	3.0
12.75	Dsz-5	20±5	3.02±0.11	256.10±1.44	9	254.99±10.25	9	84.7	3.1	84.4	4.6
13.40	Dsz-6	20±5	3.75±0.13	287.32±7.34	9	292.44±10.44	9	76.6	3.3	78.0	3.9
15.35	Dsz-7	20±5	2.76±0.11	454.46±4.13	9	425.35±14.23	9	164.0	7.0	154.0	8.0

n = number of aliquots used for equivalent dose estimation

Supplementary Table

Table S1. AMS radiocarbon data of international standards measured with samples Dsz-Ch1 and Dsz-Ch2

Standard	Type of material	Lab code	Reference ^{14}C activity (pMC)	S.E.	Measured ^{14}C activity (pMC)	±1σ	^{14}C age (a BP)	±1σ
IAEA-C1 carbonate ref.	marble	DeA-2932.1.1	0.00	0.02	0.31*	0.01	46518	362
IAEA-C1 carbonate ref.	marble	DeA-2932.2.1	0.00	0.02	0.35*	0.01	45497	335
IAEA-C2 carbonate ref.	travertine	DeA-2933.1.1	41.14	0.03	41.23	0.17	7118	34
IAEA-C9 wood ref.	kauri wood	DeA-2934.1.1	0.12-0.21		0.53	0.04	42117	555

Abbreviation: pMC = percent Modern Carbon

*No blank subtracted